ADDIS ABABA UNIVERSITY

ADDIS ABABA INSTITUTE OF TECHNOLOGY

SCHOOL OF ELECTRICAL AND COMPUTER ENGINEERING

Study on Pantograph Arcing and Investigation of its Influencing Parameters: Case Study-Addis Ababa Light Rail Transit

By

Dawit Seboka

Advisor

Abi Abate (Msc)

A Thesis Presented to Addis Ababa University, Addis Ababa Institute of Technology In Partial Fulfillment of the Requirements for the Degree of Masters of Science in Electrical Engineering (Railway)

April, 2016

Addis Ababa, Ethiopia

ADDIS ABABA UNIVERSITY

ADDIS ABABA INSTITUTE OF TECHNOLOGY

SCHOOL OF ELECTRICAL AND COMPUTER ENGINEERING

Study on Pantograph Arcing and Investigation of its Influencing Parameters: Case Study-Addis Ababa Light Rail Transit

By

Dawit Seboka

April, 2016

APPROVAL BY BOARD OF EXAMINE

_____	_____
Chairman, Department of Graduate Committee	**Signature**
_____	_____
Advisor	**Signature**
_____	_____
Internal Examiner	**Signature**
_____	_____
External Examiner	**Signature**

DECLARATION

I hereby declare that all information in this document has been obtained and presented in accordance with academic rules and ethical conduct. I also declare that, as required by these rules and conduct, I have fully cited and referenced all material and results that are not original to this work.

Dawit Seboka _____

Name Signature

Addis Ababa, Ethiopia April, 2016

Place Date of submission

This thesis has been submitted with my approval as a university advisor.

Ato Abi Abate _____

Advisor's Name Signature

ACKNOWLEDGEMENTS

I would like to express my gratitude and deep appreciation to my advisor, Ato Abi Abate, for his valuable comment, suggestions and advice during preparing this thesis. I would like to thank all the staffs of the School of Electrical and Computer Engineering at AAiT, Addis Ababa Light Rail Transit (LRT) project office staffs and my colleagues, for providing me all the invaluable materials and helpful pieces of advice.

My acknowledgment also extends to Ethiopian Railway Corporation for providing this educational opportunity.

Finally, I wish to thank my wife for her persistent support during my thesis work.

ABSTRACT

In electrified railways sliding contact between pantograph and overhead contact wire is one of the main modes of power feeding to the electrical drives and propulsion system within the railway. The traction supply could be either AC or DC at different voltage levels. Arcing from the pantograph is a commonly observed phenomenon and also the major source of Electromagnetic Interference (EMI) in the electrified railway system.

This thesis presents the study of pantograph arcing and investigation of its influential parameters for the case of Addis Ababa Light rail transit (AA-LRT). The contact between the pantograph and the contact wire is the focus point for the design of an electrified railway system in order to keep the proper contact between them.

The pantograph-overhead contact system is the system of electrified railway which is the place where pantograph arcing occurs due to the contact loss. The effects of contact distance, the weather condition, the vibration of the contact wire and the speed of the vehicle are simulated using MATLAB based on the mathematical modeling presented of this system and then analyzed for the case of AA-LRT. As the result, the weather condition and the speed of the vehicle has no any effect on the occurrence of arcing. In the case of contact distance, pantograph arcing occurs if the separation of the pantograph is not greater than 0.25mm. However, the effect of vibration of the contact wire has been found a serious cause for pantograph arcing. The pattern of the vibration is simulated for different span length (20m, 30m, 50m) and the weight of the catenary. In order to avoid the contact loss produced by the vibration of the contact wire, the minimum distance between two consecutive pantographs shall be 167 meters.

Finally, it has been recommended that the railway company running the AA-LRT will not send its vehicles uncoupled so as to avoid the effect of the front pantograph onto the next pantograph.

Keywords: Pantograph, Catenary system, Electric arc, Pantograph arcing

CONTENTS

LIST OF FIGURES

LIST OF TABLES

LIST OF ABBREVIATIONS AND SYMBOLS

AA-LRT	Addis Ababa Light Rail Transit
AC	Alternating Current
AIS	Air Insulated Substation
CZC	Current Zero Crossing
DC	Direct Current
DOF	Degree of Freedom
EMC	Electromagnetic Compatibility
EMI	Electromagnetic Interference
EW	East-West
GIS	Gas Insulated Substation
HSCB	High Speed Circuit Breaker
HV	High Voltage
LRT	Light Rail Transit
LV	Low Voltage
Mc	Motor Car
NS	North-South
OCS	Overhead Contact System
RMS	Root Mean Square
STP	Standard Temperature and Pressure
Tp	Trailer Pantograph
TPLS	Traction Power Line Substation
TRV	Transient Recovery Voltage
ω	angular frequency
ζ	damping ratio
α	mass proportional damping coefficent
β	the stiffness proportional damping coefficient
T_{CW}	Tensile force of the contact wire
T_{CA}	Tensile force of the catenary wire
v	Speed of the vehicle
f	frequency
g	arc conductance
τ	arc time constant

k	stiffness coefficient
e	elasticity
F_m	mean contact force
F_s	Static contact force
V_B	breakdown voltage
l	span length
c_w	wave propagation speed

Chapter 1

BACKGROUND AND MOTIVATION

1.1 Background

Railway transport occupies a significant role in the transport system of a country because the development of trade, industry and commerce of a country largely depends on the development of railways. The rail transport is better organized than any other form of transport. It has fixed routes and schedules. Its service is more certain, uniform and regular as compared to other modes of transport. It facilitates long distance travel and transport of bulky goods which are not easily transported through motor vehicles.

In all electrified railways, where power has to be drawn to the locomotive from outside traction power infrastructure through the pantograph on the roof of the train, there exists a sliding contact between the train and the power feeding conductor. This sliding contact between catenary and pantograph has to transfer a large amount of current and power to the locomotive reliably [2]. Pantograph arcing is the common phenomena when the pantograph head and contact wire have sliding electrical contact. This arcing is the main source of electromagnetic emissions that distorts the regular waveform of the supply voltage and current and generates transients which propagate along the railway system [1]. So, these transient electromagnetic fields affect the reliability of the associated signaling and communication systems and also disturb the function of any electronic equipment near the railway infrastructure. In addition to this, transient electromagnetic fields are produced in the signaling system when the train leaves the neutral section of the overhead power line and enters the powered section. [1]

Electromagnetic interference (EMI) is a phenomenon of the propagation of unwanted electromagnetic signals into electrical circuits of an electronic device, which may degrade the performance of the device. On the other words, electromagnetic interference is defined to exist when undesirable voltage or currents are present to influence adversely the performance of an electronic circuit or system. Interference can be intra system (within system), or it can be inter system (between systems). The system is the equipment or circuit over which one exercises design or magnetic control.

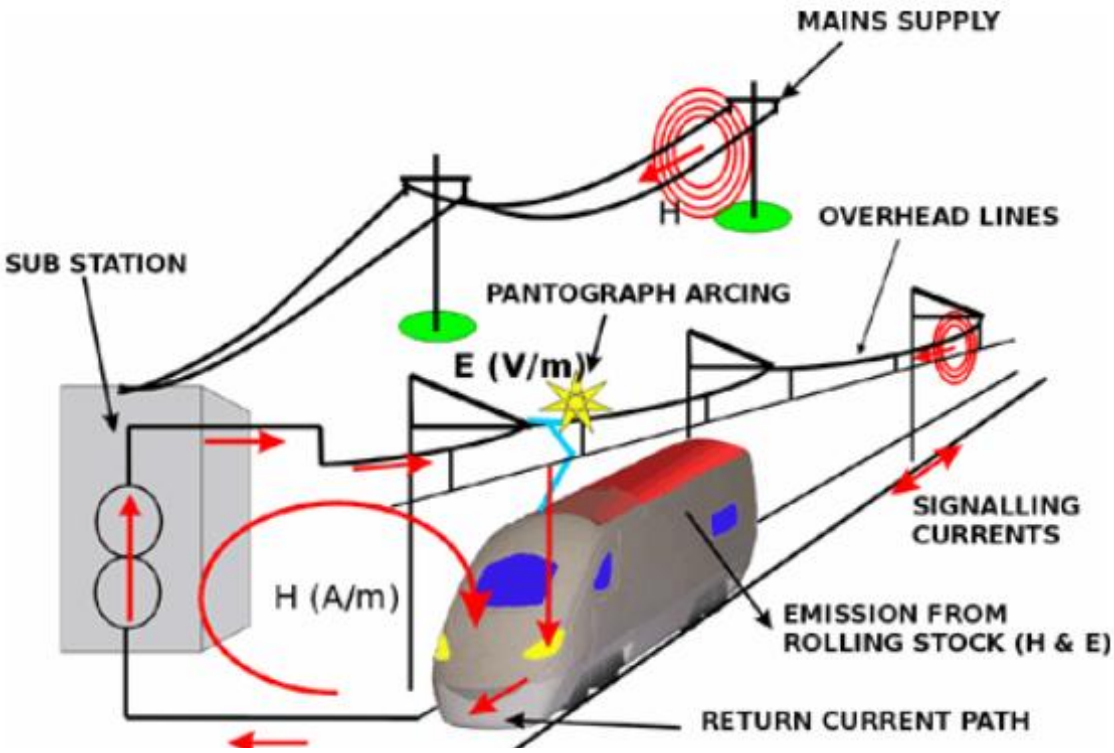

Figure 1.1: Different types of disturbance in electrified railway system

Understanding the electromagnetic emission from the railway environment is important to prevent and control electromagnetic interference. As depicted in Figure 1.1, EMI covers a wide range of phenomena, including inductive noise in parallel communication lines, impulse noise from lightning and traction transients, the production of hazardous voltage under step and touch conditions, and the appearance of stray currents. Currently, trains are more and more often equipped with potentially sensitive systems from an electromagnetic compatibility point of view. Consequently, railway systems have to be sufficiently robust to guarantee the safety of the railway transportation [7].

In this thesis, the interaction of pantograph-catenary system has been discussed and the dynamic model of this interaction is established and also disconnection events will be discussed. Electric arc modeling is discussed and simulated and then the influencing parameters of pantograph arcing are investigated and discussed.

1.2 Statement of the Problem

The pantograph arcing is the main source of broadband-conducted and radiated electromagnetic interference (EMI) for vehicle as well as traction power and signaling systems by distorting the regular waveform of the supply voltage and current and generates transients which propagate along the railway system [1]. Arcing, even though its intensity is different one railway system from another, is the common and unavoidable problems in the railway system. So, it is also the problem of the newly built AA-LRT. In order to reduce this problem and its impacts, investigation has to be made on the parameters that causes pantograph arcing.

This thesis studies about the characteristics of pantograph arcing and investigates how different operational parameters like traction current, speed of the train, and supply voltage influence the arcing and the intensity of arcing for the case of AA-LRT and then finally recommends mitigation measures.

1.3 Objectives

General Objective

The general objective of this thesis is to study pantograph arcing and investigate the influencing parameters that cause pantograph arcing.

Specific Objective

The specific objectives are:

- To investigate pantograph, overhead contact line and their interaction.
- Theoretical understanding of the event and influencing parameters on pantograph arcing and its characteristics.
- To explain the effects of pantograph arcing on traction power and signaling systems.
- To investigate possibility of vibration of the contact wire between successive pantographs.
- To investigate different parameters such as speed of the vehicle, contact force, and weather conditions on pantograph arcing.
- To recommend the mitigation measures to be taken for reducing the occurrence of pantograph arcing.

1.4 Methodology

In order to achieve the objective of the thesis, different procedural tasks are followed. The first method towards processing the work is started with reviewing different literatures where all the theoretical information regarding the pantograph arcing and pantograph-catenary contact system is reviewed. Alongside with literature reviewing, the collection and verification of data for the analysis is performed. This is followed by studying the characteristic and system modeling of the pantograph arcing and the parameters that influences it. Once the model is developed using MATLAB, the analysis of the system is performed. Finally, the influence of different parameters will be analyzed. The general block diagram of the methodology is given below.

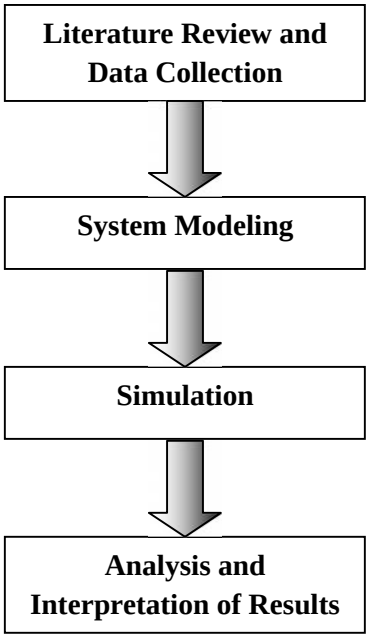

Figure 1.2: Methodology diagram

1.5 Scope of the Study

The investigation will be based on simulation of the characteristics of the pantograph arcing as prototype implementation is not feasible. In as much as possible, an attempt will be made to drive analytical expression that will help to support the simulation. The core of the work, which is investigation of the event and influencing parameters on pantograph arcing and its characteristics; requires knowledge of the AA-LRT systems.

1.6 Literature Review

Because of its limitation on railway and nearby environment, pantograph arcing have got a wide research attentions in the last few years. Some of the researches conducted on the area pantograph arcing and related to this work are briefly reviewed below.

In [1], the authors investigated EMI generation from pantograph arcing using two phases. Different possible mechanisms of the pantograph arcing and influencing parameters like speed of the train, load current, voltage level, power factor etc. are identified by experimental investigations done in the first phase. Transients and asymmetrically distorted voltage and current waveforms are generated due to the pantograph arcing. The characteristics of this high frequency emission and influencing parameters have been analyzed and presented in the second phase of this thesis. Measurements of radiated emissions have been conducted at a distance of 10 m from the center of the track. Finally, the paper describes how the wideband electromagnetic emission to influence on the function of traction power, signaling and train control systems. And then put some mitigation techniques to overcome these effects.

In [2], the pantograph arc impedance is modeled by taking arc voltages as output and experimental arc currents as an input differentiating each other by the RMS value, the voltage level, the power factor or the speed of the train. The experiment has been performed notably for 50Hz AC. This thesis presents the analysis of this data, in order to define and create a model for the arc impedance. The paper studied 16 test runs which have different characteristics, like speed of the train, load current, voltage level and power factor. Based on this, an impedance model has been built. Once the model has been built, the following points are investigated:

- The simulated arc voltages were quite similar to the experimental voltages and
- The arc current is to be the main part of the information about the arc phenomenon.

In addition to this, the transient overvoltage as well as the average values is well modeled and approximated. Finally, an electric circuit model is elaborated. Starting from a simple frequency analysis, an RLC circuit has been simulated.

In general, in order to reduce impact of Electromagnetic interference, it is valuable to deal the cause and develop mitigation scheme for it. This paper investigate one of the main source of Electromagnetic interference, i.e. Pantograph arcing.

In [3], the analysis of pantograph arcing and its effects on the railway vehicle is presented. Sliding contact between the pantograph contact strips and the catenary contact wire is described with the emphasis on the pantograph arcing. Electric arc is examined in details. Arc characteristics, formation methods, extinction and reigniting of the arc are studied. An experimental test setup is designed and implemented to be used in this work. Outputs of the experiments are presented and discussed. Arc models and theories are examined in details. Basic arc models in ATP-EMTP are studied and a suitable arc model for pantograph arcing is generated and validated with experimental results. Contactless inductive power transfer and usage of super capacitors in electric trains are also discussed.

1.7 Organization of the Thesis

The study and the investigation of influencing parameters of pantograph arcing is presented in this thesis. In order to achieve this, the paper is organized into six chapters. The detailed outlines are as follows:

Chapter 2 discusses about the Addis Ababa light rail transit. In this presentation, the technical specification of its different systems related to the interaction of the pantograph and catenary are discussed.

Chapter 3 discusses about sliding contact between pantograph and overhead contact wire. In this chapter the theoretical background of pantograph, catenary system and their dynamic characteristics are presented. Furthermore, the concept of electric arc is examined based on the arc produced in the high voltage circuit breaker. Following this, the pantograph arcing, its effects and arc modeling are discussed.

In Chapter 4, the mathematical modeling and analysis of pantograph arcing and pantograph-catenary contact system are discussed.

In the fifth chapter of this thesis, simulation result using MATLAB is shown.

Chapter 6 The conclusions drawn from the research work, recommended solutions are included in this chapter.

Chapter 2

OVERVIEW OF ADDIS ABABA LIGHT RAIL TRANSIT

2.1 Introduction

Addis Ababa is not only the capital city of Ethiopia but also the seat for the Africa Union and the Africa Economic Commission. The increasing expansion of the traffic congestion and the population of the city, its transportation system are demanded the transformation of buses and taxis to light rail transit. Hence, AA-LRT is the way to finalize its project phase and it is expected to start operation in this month. In this chapter, the technical parameters of the design and construction of the AA-LRT especially its power supply system and overhead contact line is briefly introduced. Furthermore, the summary of technical specification the light rail vehicle that is involved in the operation is presented.

Addis Ababa Light rail Transit is composed of the East-West and North-South lines. Modern tram cars are adopted. Most of the tracks are constructed on the ground, and some sections are built on overhead bridge or in underground tunnels. 15kV diversified power supply system is adopted. For the traction power supply system, DC750V overhead contact system (OCS) and running rail return mode are adopted for the power supply.

The East-west (Phase I) starts from the south side of gate of Tor Hailtoch Hospital in the west. It runs through the Mexico Square, the Mesekel Square and the Megenagna and finally runs to the Ayat. This line has the subgrade section about 12.896km in length, the elevated section about 3.904km in length (including a common rail section 2.662km in length), and underground section 0.197km in length. Totally 22 stations are set; wherein, 6 elevated stations (including 5 shared track stations) and 2 semi-underground stations are included and the rest stations are ground stations. The maximum distance between stations is 1.26km, the minimum distance between stations is 0.435km and the mean distance between stations is 0.798km.

Figure 2.1: AA-LRT line map

The South-north Line Phase I Project starts from the east side of St. George Church in the north. After it is laid in a section along the north side of Mercato Market, it turns to the south. After it runs through the west side of this market to the Chad St. and connects the track of the East-west Line, it is laid to the east. It runs to the west side of Meskel Square and turns to the south. It goes through the Meshalokia Bridge and then takes the way under Gotera interchange Bridge and finally it runs to the Kality. The length of roadbed section in the South-north Line is approximately 10.057km, the length of elevated section is approximately 5.977km (including the 2.662km shared track section) and the full length of underground section is approximately 0.655km. Totally 22 stations are set; wherein, 8 elevated stations (including 5 shared track stations) and 1 underground station are included and the rest stations are ground stations. The maximum distance between stations is 1.972km, the minimum distance between stations is 0.435km and the mean distance between stations is 0.773km.

2.2 Power Supply System

The power supply system of the Addis Ababa Light rail transit includes four main substations, which are gas insulated substation (GIS) and air insulated substation (AIS), 19 traction rectifier units or Traction Power Line Substation (TPLS). The four main substations receive power AC132kV from the national grid and step-down it to AC15kV in order to feed the TPLS. The TPLS rectifies and transforms this power and sends DC750V to the overhead contact system. It

has a 12-pulse rectification. The power factor is greater than 0.95 when at rated load. The rated capacity of traction rectifier transformer is about 1.5MW. The range of voltage fluctuation on the overhead contact line is DC 500-900V.

2.3 Overhead Contact System (OCS)

Traction power for train operation can be either generated on board or collected from overhead wire or third rail. It is necessary an appropriate power collecting mechanism for the case of overhead wire or third rail. The power collection mechanism for Addis Ababa LRT is overhead contact system.

The catenary suspension of AA-LRT uses all auto-tensioned simple catenary equipments with wire composition of twin catenary and contact wire for the main line. The rated tension of both Catenary and contact wires is 12kN. Moreover, the zigzag section of straight section is ±200mm in general. It uses 30-50 meters span length depending on the curve radius the line.

The main technical parameters of the overhead contact system of Addis Ababa light rail transit are shown in the table below:

Table 2.1: Technical parameters of OCS of AA-LRT

S.N.	Description	Contact wire	Catenary wire
1	Wire type	Silver-copper alloy (CTAH150)	Copper strand (JT150)
2	Nominal cross-sectional area	150 mm^2	150mm^2
3	Unit mass for reference	1.35 kg/m	1.342 kg/m
4	Resistivity at 20^oC	$1.777x10^{-2}$ $W.mm^2/m$	
5	Resistance temperature coefficient	$3.81x10^{-3}/K$	
6	Current carrying capacity at 95^oC	580A	580A
7	Linear Expansion Coefficient	$1.7x10^{-5}/K$	$1.7x10^{-5}/K$

2.4 Rolling Stock

The vehicles shall be 70% low-floor articulated 6-axle modern trams, consisting of three modules, bi-directional driving. Two tramcars shall be able to operate with double heading. Train formation of the LRT vehicle is Mc + Tp + Mc , where Tp = Trailer pantograph and Mc = Motor car. The Mc module is a motor module for installation of motor, bogies and driver's cab. Whereas, Tp module is trailer module for the installation of pantograph and trailer bogies.

Figure 2.2: The light rail vehicle of AA-LRT

The high voltage traction system of whole vehicle has the following parts: pantograph, arrester, high-speed circuit breaker, traction inverter, traction motor and brake resistance. The basic working principle of traction system is that the power of pantograph is supplied by 750V DC power of contact net, which connects to traction inverter by high speed circuit breaker (HSCB). The opening and closing of main traction circuit is controlled by HSCB. Each MC vehicle is equipped with a traction inverter, which is to supply power to the two traction motors on bogie.

A pantograph is set on trail car to supply the rated DC750V high voltage power of grid to high voltage equipment of vehicle; main circuit system is an effective carrier to realize train traction power and electrical brake force, meanwhile, the power of other train systems is also from main circuit system, to make sure the equipment safety of vehicle high voltage system, the train is equipped with surge absorption high voltage protection equipment (arrester), for protection of high voltage power circuit equipment of train.

Addis Ababa light rail transit adopts the CED125D type single arm pantograph. The technical parameters of this pantograph are:

- Temperature of working environment: -35^{o}C to 65^{o}C
- Slide board length: 1047mm

- Slide board material: the metal impregnated carbon
- Control voltage: DC24V
- Control current: max 13A
- Working width of pantograph: 1300mm
- Width of the pantograph head: 1900mm
- Contact Pressure: 60 to 140N
- Nominal speed: 120km/h
- Nominal system voltage: DC1500V
- Operation current: 1050A

The following are the parameters of specifications of the Addis Ababa Light Rail Vehicle:

- Number of coaches per train: 3
- Car capacity: 286 passengers or 306 passengers
- Car weight at full load: 63.02 tones
- Operational speed: 21.6 km/h to 30km/h
- Maximum speed : 70km/h
- Trains in operation: 41
- Train Spacing: 2.16 km
- Headway: 6 minutes if all the trains are in operation.

Chapter 3

PANTOGRAPH-OVERHEAD CONTACT SYSTEM

3.1 Introduction

Contacts between pantograph and catenary are the most critical parts in the transmission of electrical energy for electrified trains. The dynamic performance of a pantograph-catenary system plays an important role in maintaining good contact between the pantograph and catenary and improving the quality of current collection. The lack of good contact between them is the cause of pantograph arcing. In this chapter, a brief review of pantograph, overhead contact system and dynamic parameters of their contacts are presented.

In electrified railway system, there are different subsystems that contribute for supplying power to the locomotive. Among these subsystems, the major subsystems are the traction power substation, the overhead line, pantograph and the traction motor. The substation and the overhead line are off-board subsystems whereas pantograph and the traction motor are on-board power equipments. Pantograph-overhead contact is the power interface of the on-board and off-board power subsystems. The following figure shows the block diagram of this system.

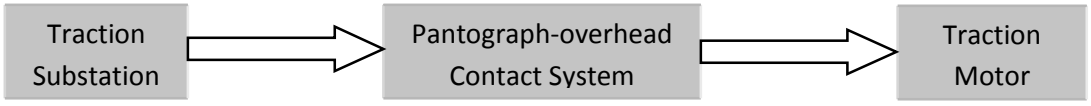

Figure 3.1: The block diagram of the electrified railway system

Traction Substation: It is the system used to transform the externally received power to the power required to the railway system and transfer it to the overhead contact system.

Pantograph-Overhead Contact System: In this system, the power is transferred to the motor by the sliding contact of the pantograph with the contact wire. The contact wire and the pantograph are unrelated but they are interrelated and interacted with each other by the uplift force due to the pantograph. The quality or the performance of the contact is the very interesting thing for the proper movement of the train. The pantograph-overhead contact is also the place where pantograph arcing is occurred.

Traction Motor: This motor receives power collected by the pantograph and converts this electrical power to mechanical energy and makes the vehicle movement.

Pantograph

Railway traction is a complex mix of electrical and mechanical parameters. Pantograph acts as an active link between the catenary and electric drive used for driving the electric locomotive. It is a device that collects electric current from overhead lines and supplies it to locomotive transformer for feeding to the drive. It is a mechanical system composed of an articulated frame, carrying a collector head on which the collector strips for current collection are mounted. Constant pressure is applied at the head of the pantograph through pneumatic control mechanism to ensure that it always remain in contact with the contact wire. When the electric train moves, a dynamic force is applied on the contact wire by the head of the pantograph.

The pantograph is a spring loaded device which pushes the contact wire in order to collect power required for the train. The contact shoe starts sliding over the wire whenever the train moves. This can set up acoustical standing waves in the wires which break the contact and interrupt power collection. Therefore, the force applied by the pantograph to the catenary is used to avoid loss of contact due to excessive transient motion.

Different types of pantographs are used depending on the train model and adapted traction system. Two common types of pantographs are: [1]

1. Double armed (sometimes called Diamond shaped) and

2. Single armed (sometimes called Z-shaped or half pantograph)

Double arm or Diamond shaped pantographs are usually heavier, requiring more power to raise and lower, but may also be more fault tolerant. On railways of the former USSR, the most widely used pantographs are those with a double arm ("made of two rhombs"), but since the late 1990s there have been some single-arm pantographs on Russian railways. Some streetcars use double-arm pantographs, among them the Russian KTM-5, KTM-8, LVS-86 and many other Russian-made trams, as well as some Euro-PCC trams in Belgium [8].

The most common type of pantograph today is the so called half-pantograph (sometimes 'Z'-shaped), which has evolved to provide a more compact and responsive single-arm design at high speeds as trains get faster. The half-pantograph can be seen in use on everything from very fast trains to low-speed urban tram systems. The design operates with equal efficiency in either direction of motion, as demonstrated by the Swiss and Austrian railways whose newest high performance locomotives, the Re 460 and Taurus respectively, operate with them set in opposite directions [8].

Figure 3.2: Single arm or Z-shaped pantograph [4]

Catenary System

The catenary system is the wiring structure of the overhead contact system that consists of a contact wire, a messenger wire and droppers. Electric trains draw current through the contact of its pantograph with the contact wire which is the underside of the lowest wire of an overhead contact system. To achieve good current collection, it is necessary to keep the contact wire geometry within defined limits. This is usually achieved by supporting the contact wire from above by a second wire known as the messenger wire or catenary. This wire supports the contact wire by means of droppers. The messenger wire is supported regularly at structures, by a pulley, link, or clamp. The whole system is then subjected to a mechanical tension. Overhead contact line is commonly classified as simple, stitched and compound catenary according to the design of the tensioning system used.

Simple Catenary: - It is characterized by either a dropper connecting the contact wire to the catenary wire at or in the immediate vicinity of the support, or droppers at a distance of 2.5 to 10 meters from the support points where introduced between catenary wire and contact wire.

Compound Catenary: - A compound catenary has a second catenary wire, called the auxiliary catenary wire between the main catenary wire and the contact wire. It is jointed to the main catenary wire and the contact wires by means of droppers which help to eliminate variations in elasticity.

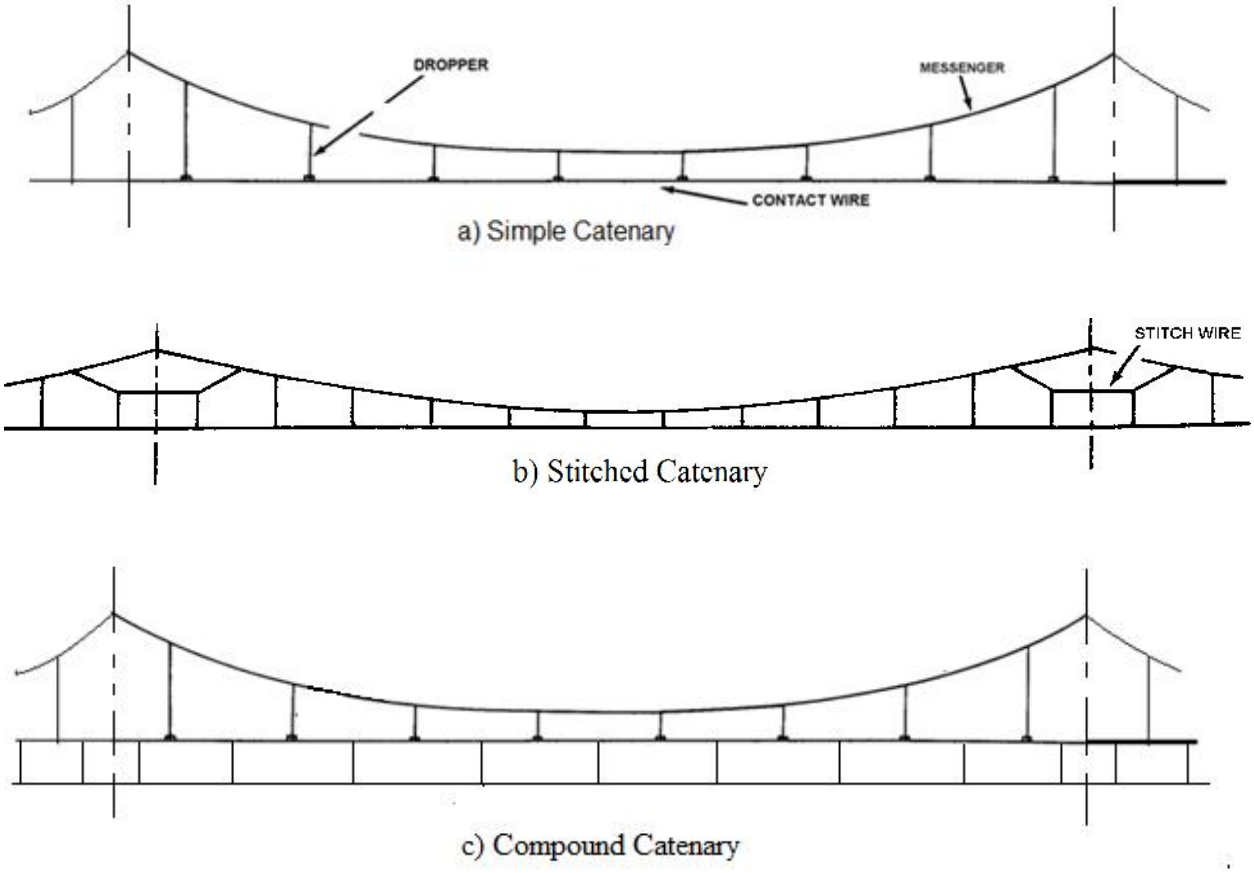

Figure 3.3: Different types of catenary system

Stitched Catenary: - The term stitch wire is used to designate a connecting element that added to each support structure, terminated on the either side of the catenary wire.

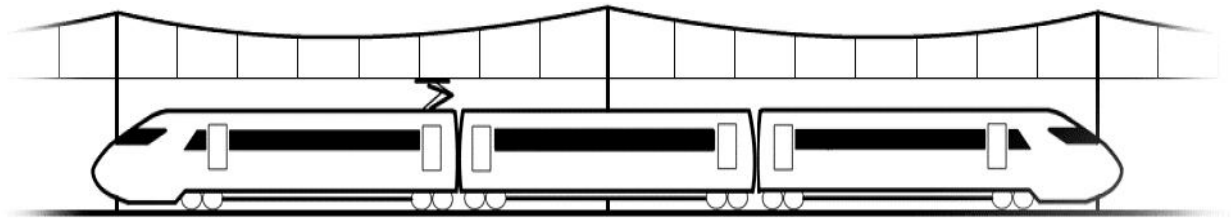

Figure 3.4: A train with its catenary-pantograph system

3.1 Contact Force and Uplift of Contact Wire

Contact Force

The interaction of interoperable pantographs with interoperable overhead contact lines forms an aspect for which a set of requirements was stipulated concerning the static contact force, the mean contact force and the quality of current collection. The measurement of contact forces is one of the approaches specified for the assessment of the components and subsystem.

If the contact force is too high the contact will be well insured, but it will lead to undesirable rapid wear on the carbon collector strips. If the magnitude of the contact force is too low, there is poor contact and create loss of contact due to dynamic effects. This loss of contact produces arcing. Thus the magnitude of the contact force is an interesting parameter to investigate. The quality of dynamic interaction performance can be measured by [15]:

- The contact forces characterized by mean value, standard deviation and maxima and minima; or
- The percentage of arcing.

Static Contact Force

The static contact force is the mean vertical force exerted upward by the collector head on the contact wire, and caused by the pantograph raising device whilst the vehicle is at standstill.

Table 3.1: Static contact forces in N [15]

	Nominal Value	Range for application for upgrading
AC	70	60 to 90
DC 3KV	110	90 to 120
DC 1.5 KV	90	70 to 110

Mean Contact Force

In running situations the contact force varies according to many factors such as elasticity, the static force used, where the pantograph is along a span and which speed the train travels at. The mean contact force F_m is formed by the static and aerodynamic components of the pantograph contact force with dynamic correction.

$$F_m = \sim . v^2 + F_s \tag{3.1}$$

Where: v is the velocity of the train in *km/h*

α is the uplift coefficient

F_s is the static contact force

The first term in equation 3.1 represents the aerodynamic force, while the second term represents the static uplift force of the pantograph. Range of the contact force, $F_m \pm \pm_m$, where σ_m is the contact force standard deviation.

Uplift of Contact Wire

The pantograph and the contact wire are interacted with each other by means of uplift force or contact force. The uplift force is caused by the pantograph in order to make contact to the catenary system to draw current for the motor where as the contact force is the reaction of the contact wire. When the running pantograph is passing by the relatively static catenary, the contact wires suffer from external interference, so a dynamic interaction is generated between the pantograph and the catenary. As the speed increases, vibration become serious, and can force the pantograph slide away from the contact wires and generate arcs and sparks. The non-linear characteristics of arcs between the pantograph and the catenary causes line voltage distortions.

Moreover, the contact loss is directly affect the current collection, and even cause instantaneous power supply interruptions, which cause a loss of train traction and braking force.

Elasticity is a measurement of how flexible the catenary system is in the vertical direction. This is measured in how many millimeters the contact wire is pushed upwards per Newton. The elasticity, *e*, at the middle of a span can be obtained using the equation [15]:

$$e = \frac{l}{k'(T_{CA} + T_{CW})} \tag{3.2}$$

Where:

l is longitudinal span in m;

T_{CW} is contact wire tensile force in kN;

T_{CA} is catenary wire tensile force in kN;

k' is numeric factor ranging between 3.5 and 4.0.

The elasticity at supports, contact lines without stitch wires achieve an elasticity of only 30% to 50% of the midspan values. However, by adding suitable stitch wire arrangements, the elasticity at the supports can be increased to approximately 90% of the mid span values.

The traction vehicle bearing the pantograph is at standstill or travels only slowly, the dynamic effects can be neglected and the uplift y_o at the point of contact is equal to the product of the contact wire force F_o and elasticity *e* of the contact wire [15].

$$y_o = F_o e \tag{3.3}$$

The uplift curve of the contact wire is symmetrical about the position of the pantograph and the length of the uplifted contact wire, l_y is [15]:

$$l_y = \frac{F_o}{m'g} \tag{3.4}$$

Where *m'* is mass per unit length of the catenary structure.

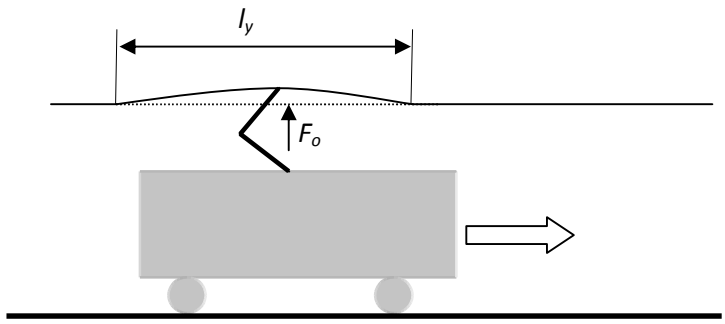

Figure 3.5: Train with pantograph moving along a contact wire

A useful model for studying the behavior of contact wire is achieved by treating the contact wire as a tensioned string without bending stiffness or as a flexible beam.

The uplift of an overhead contact line should be kept to a minimum in order to achieve good contact quality. However, a certain amount of elasticity is required. The mechanical design of the supports limits the possible vertical contact wire uplift at the supports. At low and medium speeds, i.e. at speeds of up to approximately 50% of the wave propagation speed, the uplift is proportional to the elasticity of the overhead contact line and the contact force exerted by the pantograph. To maintain a favorable contact quality at increasing speeds, the contact force needs to be increased as well. Therefore, the elasticity has to be kept as low as possible to limit the resulting uplift.

3.2 Dynamic Characteristics of Overhead Contact Line

Dynamic characteristics of overhead contact line designs include the natural frequencies, *f*, the wave propagation speed, c_w, the reflection coefficient, *r*, the Doppler factor, df, the amplification coefficient, γ_A , and damping. [21]

The Natural Frequencies of Catenary Systems

The natural frequencies of the catenary system are numerous because of it has many degree of freedoms (DOFs) and there can be calculated one frequency for each DOF.

If the oscillation is assumed to be a stationary wave, the frequency f_1 can be calculated as [21]:

$$f_1 = \frac{c_w}{2l} = \frac{1}{2l}\sqrt{\frac{T_{CW} + T_{CA}}{m'_{CW} + m'_{CA}}} \tag{3.5}$$

Here c is the mean wave propagation speed (m/s), l is the span length (m), f_1 is the first natural frequency (Hz); T_{cw} is the tensile force in the contact wire (N), T_{CA} is the tensile force in the messenger wire (N), m'_{cw} is the mass per unit meter in the contact wire (kg/m) and m'_{CA} is the mass per meter in the messenger wire (kg/m).

The Wave Propagation Speed

The wave propagation speed, c_w, is the speed of a transversal impulse i.e. the local vertical movement caused by the pantograph moving. If the train speed is so high that it catches up with the impulse the wire will get an infinite large vertical displacement [21].

The wave propagation speed can be expressed as [1]

$$c_w = 3.6\sqrt{\frac{T_{CW}}{m'_{CW}}} \tag{3.6}$$

Where, c in km/h;

T_{CW} is tensile force in contact wire, N;

m'_{CW} is mass per unit length of contact wire, kg/m.

The Reflection Coefficient

The reflection coefficient, r, is defined as [3].

$$r = 1/\left(1+\sqrt{\frac{T_{CW}.m'_{CW}}{T_{CA}.m'_{CA}}}\right) \tag{3.7}$$

Where T_{cw} is the longitudinal force (N) in the contact wire, T_{CA} is the longitudinal force (N) in the messenger wire; m'_{cw} is the mass per meter (kg/m) for the contact wire and m'_{CA} is the mass per meter (kg/m) for the messenger wire.

The Doppler Factor

The Doppler factor, df, is a factor which approaches zero as the velocity of the train approaches the wave propagation speed [15].

$$df = \left(\frac{C_{CW} - v}{C_{CW} + v} \right) \tag{3.8}$$

The Amplification Coefficient

The amplification coefficient, γ, shows whether the change in the contact force will be less or more than the previous time the pantograph hit a reflecting transversal wave as the pantograph approaches the source of the reflection, e.g., a dropper. The amplification coefficient can be computed as [15]:

$$¥_A = r/df \tag{3.9}$$

Damping of Catenary Systems

The catenary system is a structural system with very light damping thus the damping characterization is important. The damping of the catenary system is included as Rayleigh damping [21]. It is usual to include the damping as proportional damping, such as Rayleigh damping. The Rayleigh damping matrix defines the global damping matrix as a linear combination of the mass matrix and the stiffness matrix [22].

$$[C] = \sim .[M] + \quad .[K] \tag{3.10}$$

To obtain values for α, the mass proportional damping coefficient, and β, the stiffness proportional damping coefficient, the natural frequencies of the global system had to be identified. Then the first natural frequency and a frequency a little lower than the maximum frequency of interest were used to be computed them as shown in the formula below [22]:

$$\sim = ¸ \frac{2\mu_1\mu_n}{\mu_1 + \mu_n} \quad and \quad = ¸ \frac{2}{\mu_1 + \mu_n} \tag{3.11}$$

ζ is the damping ratio, ω_1 is the first natural frequency (rad/s) and ω_n is the higher frequency (rad/s). The motivation for choosing ω_n is as close to the highest frequency of interest and not the highest which this gives a more correct damping throughout the whole range of frequencies [22].

3.3 Electric Arc

The electric arc between the pantograph contact strips and the overhead line is similar to the electric arc in a circuit breaker. In both situations the electric arc is formed by separation of the contacts. Although there are lots of researches and experiments on the electric arc in a circuit breaker, there are a few researches on the pantograph arcs. Therefore, previous studies on the electric arc in circuit breakers may be useful to understand the pantograph arcing.

It has been known that all gases are normally good electrical insulators. But, the application of a sufficiently high electrical field may cause breakdown of the insulating properties which leads to large currents passing through the gas. The phenomena associated with the passage of the current, which is called an electrical discharge through the gas, depend markedly on the nature and pressure of the gas, on the materials of which the electrodes are made, on the geometry of the electrodes and of any containing vessel, and on the magnitude of the current flowing [3].

An electric arc is a type of gas discharge phenomenon in which current is conducted through a hot-ionized gas between an anode and a cathode. It is an electrical breakdown of a gas that produces an ongoing plasma discharge, resulting from a current through normally nonconductive media such as air. The ionized gas forms plasma which interacts with electric field produced by the current. The maximum current through an arc is limited only by the external circuit, not by the arc itself.

Characteristics of the Arc

The electric arc consists of ionized gas, and it originates and ends on small spots on the electrodes. No matter what the total arc length is, arc is composed of three distinct regions namely the cathode region, the anode region and the arc column or arc plasma region [29]. Through all these regions current is carried by electrons and ions. The electric potential distribution along the arc is plotted against the arc length in figure below.

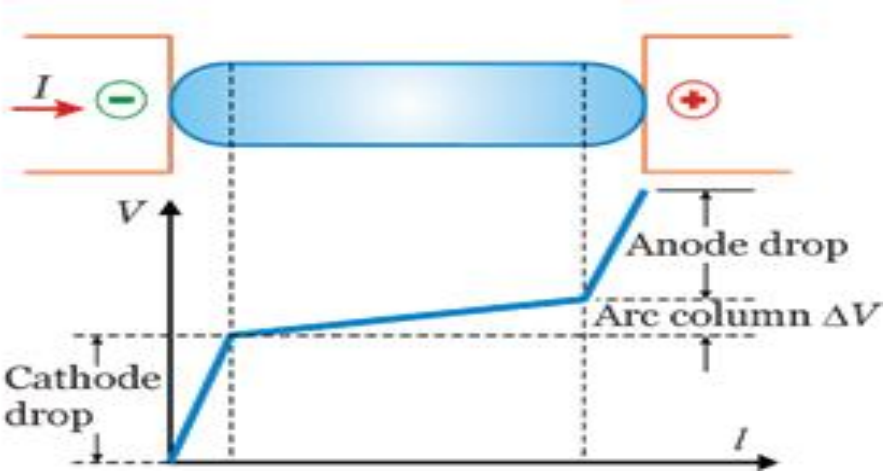

Figure 3.6: Voltage distribution of an arc [28]

Cathode region is a region adjacent to the cathode. The width of the region depends on the arc current, the medium in which it is burning and the cathode material. The function of this region is to conduct the arc current across the junction from the cathode to the arc column in a stationary way without any current divergence.

Likewise, anode region is a region adjacent to the anode. The anode has to perform two tasks which are to receive the arriving electrons and gain their energy and also to generate as many ions as disappears continuously towards the arc column, even though their number per unit time is small.

The arc column is a region, situated in between anode and cathode regions, which is electrically neutral as it contains almost equal number of ions and electrons. The ionization in the arc column is maintained by the energy dissipated in the arc. In this region, the current is mostly carried by electrons due to their small mass and high mobility. In order to have a sufficient electrical conductivity in the arc column its temperature must be very high.

The length of the anode and cathode drop regions (l_a and l_c) is small; it is of the order of micrometers, and l_a [l_c. It can be seen that the electric field strength is much higher in these regions than in the arc column [28]. If the arc length is short, the voltage along the arc column becomes negligible, only the anode and cathode drops contribute to the arc voltage.

Arc Formation

The factors that are responsible for the maintenance of arc between the contacts are:-

Potential Difference between the Contacts: When the contacts have a small separation, the potential difference between them is sufficient to maintain the arc. One way to extinguish the arc is to separate the contacts to such a distance that potential difference becomes inadequate to maintain the arc. However, this method is impracticable in high voltage system where a separation of many meters may be required.

Ionized Particles between Contacts: The ionized particles between the contacts tend to maintain the arc. If the arc path is de-ionized, the arc extinction will be facilitated. This may be achieved by cooling the arc or by bodily removing the ionized particles from the space between the contacts.

Extinction of the Arc

There are two methods of extinguishing the arc in circuit breakers. They are high resistance method and low resistance or current zero method.

***High Resistance Method*:** In this method, arc resistance is made to increase with time so that current is reduced to a value insufficient to maintain the arc. Consequently, the current is interrupted or the arc is extinguished. The principal disadvantage of this method is that enormous energy is dissipated in the arc. Therefore, it is employed only in DC circuit breakers and low capacity AC circuit breakers.

The resistance of the arc may be increased by:

i. ***Lengthening the Arc: -*** The resistance of the arc is directly proportional to its length. The length of the arc can be increased by increasing the gap between contacts.
ii. ***Cooling the Arc: -*** Cooling of the medium between the contacts increases the arc resistance.
iii. ***Reducing the Cross-section of the Arc: -*** If the area of cross-section of the arc is reduced, the voltage necessary to maintain the arc is increased. In other words, the resistance of the arc path is increased. The cross-section of the arc can be reduced by letting the arc pass through a narrow opening or by having smaller area of contacts.

iv. ***Splitting the Arc: -*** The resistance of the arc can be increased by splitting the arc into a number of smaller arcs in series. Each one of these arcs experiences the effect of lengthening and cooling. The arc may be split by introducing some conducting plates between the contacts.

***Low Resistance or Current Zero Method*:** This Method is employed for arc extinction in AC circuits only. In this method, arc resistance is kept low until current zero where the arc extinguishes naturally and is prevented from re-striking in spite of the rising voltage across the contacts. All modern high power AC circuit breakers employ this method for arc extinction.

In an AC system, current drops to zero after every half-cycle. At every current zero, the arc extinguishes for a brief moment. Now, the medium between the contacts contains ions and electrons so that it has small dielectric strength and can be easily broken down by the rising contact voltage known as transient recovery voltage (TRV).

If such a break-down does occur, the arc will persist for another half-cycle. If immediately after current zero, the dielectric strength of the medium between contacts is built up more rapidly than the voltage across the contacts, the arc fails to re-strike and the current will be interrupted. The rapid increase of dielectric strength of the medium near current zero can be achieved by:

- causing the ionized particles in the space between contacts to recombine into neutral molecules; and
- sweeping the ionized particles away and replacing them by unionized particles.

Therefore, the real problem in AC arc interruption is to rapidly de-ionize the medium between contacts as soon as the current becomes zero so that the rising contact voltage or re-striking voltage cannot breakdown the space between contacts. The de-ionization of the medium can be achieved by:

i. ***Lengthening of the gap: -*** The dielectric strength of the medium is proportional to the length of the gap between contacts. Therefore, by opening the contacts rapidly, higher dielectric strength of the medium can be achieved.
ii. ***High pressure: -*** If the pressure in the vicinity of the arc is increased, the density of the particles constituting the discharge also increases. The increased density of particles causes

higher rate of de-ionization and consequently the dielectric strength of the medium between contacts is increased.

iii. ***Cooling:*** **-** Natural combination of ionized particles takes place more rapidly if they are allowed to cool. Therefore, dielectric strength of the medium between the contacts can be increased by cooling the arc

iv. ***Blast effect:*** **-** If the ionized particles between the contacts are swept away and replaced by un-ionized particles, the dielectric strength of the medium can be increased consider-ably. This may be achieved by a gas blast directed along the discharge or by forcing oil into the contact space.

Re-ignition of the Arc

There are different types of re-ignition of the arc.

Dielectric Re-ignition**:** When the electrodes of any electrical contact open with AC supply, an arc is formed and it continues burning till the next CZC. Just after the CZC, the voltage across the electrodes keeps on rising with the line voltage and then within a few microseconds, that too is exceeded and is called transient recovery voltage (TRV). The rate of rise and amplitude of the TRV depends on the circuit parameters being interrupted, whether resistance, capacitance or inductance (or some combination).

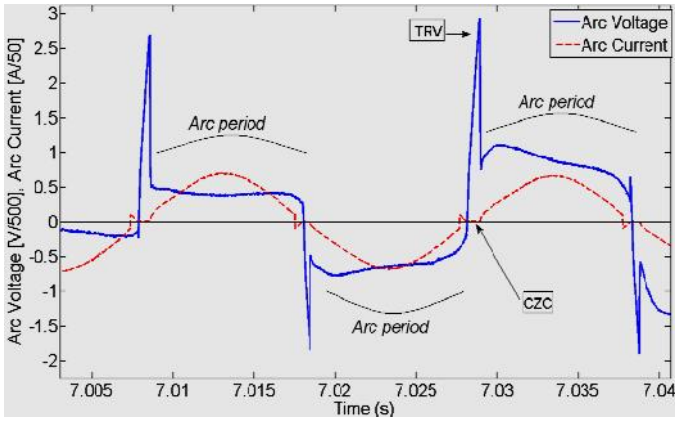

Figure 3.7: Current zero crossing (CZC) and transient recovery voltage (TRV) [2]

For extinction of the arc, the electron emission cease and all factors which enhance this process should facilitate the arc quenching. This is followed by heat loss of the arc plasma, cooling of the electrode surfaces and a slow increase in dielectric strength of the air gap. At one point of time,

the reduction in plasma temperature could be low enough (usually the critical temperature in the range of 2000-3000 K) to make thermal ionization in the plasma. Then the breakdown voltage will depend on the gap length, gas pressure, gas number density and temperature.

At this point, the transient recovery voltage (TRV) will stress the whole gap between the electrodes. A breakdown of the contact gap after CZC is followed by a current pause. The appearance of the TRV across the contact gap is called as dielectric re-ignition.

***Thermal Re-ignition*:** The cathode sheath formed by the space charges can produce field emission of electrons from the new cathode. If the TRV is higher than the cathode sheath voltage, the excess voltage will appear across the decaying plasma. These field emitted electrons from the new cathode are accelerated by the voltage drop across the plasma and heat up the arc column again. This eventually leads to a sustained current even after the CZC and is called thermal re-ignition.

3.4 Pantograph Arcing

In all electrified railways where power has to be drawn to the locomotive from outside traction power infrastructure through the pantograph on the roof of the train, there exists a sliding contact between the train and the power feeding conductor. The slide contact between the pantograph and the contact is the main system that interfaces the train with the infrastructure.

A big amount of power is transmitted through a small contact area between the overhead contact wire and the carbon blade of the pantograph. To achieve this and also provide quality power to the propulsion system requires smooth operation of the sliding contact and so, it should have the following properties [1]:

- The physical contact between the pantograph and the overhead contact wire must be maintained continuously as the train moves
- The pantograph must provide low aerodynamic resistance
- The wear of the carbon blade should be low
- The overhead contact wire should not be abraded
- Both the pantograph and the overhead contact wire should be able to withstand high current and high temperature

Even when the train is stationary, it still draws some power (80-300A depending on supply voltage as per IEC 50367:2006) and the contact should be able to bear that without being welded /joined.

In order to transfer power to the rolling stock with the required quality, it is necessary to have a proper electrical contact between the pantograph and the contact wire. Any interruption in power feeding will affect the power quality followed by service disruptions resulting in unwanted stoppage of trains. During the interaction between pantograph and contact wire, the loss of contact occurs due to different reasons and this produces pantograph arcing.

Pantograph arcing is a kind of electric arc occurred in an electrified railway when the pantograph of the locomotive losses its contact to the current carrying conductor. It is a complex phenomenon and depends on speed of the train, current, presence of inductance etc. Because of the irregularity of catenary and tracks, the vibration between catenary and pantograph and other factors during the process of power supply, it is inevitable that pantograph will separate from the contact wire. The separation of pantograph and contact wire will lead to pantograph arcing, and simultaneously it will cause the current flowing through the locomotive equipment become discontinuous. On one hand, wear of pantograph strip and catenary wire increases significantly [3]. In a sliding contact like pantograph and contact wire, the arc root moves across both electrodes because of the relative motion between them.

3.5 Effects of Pantograph Arcing

It is the most common and distorts the waveform of the supply voltage and current, generates transients and can cause interference with the traction power and signaling system. One of the effects of pantograph arcing is to distort the current waveform which contains a wide band of harmonic contents, including DC components, even harmonics and inter-harmonics. In this section, some effects of pantograph arcing specially effects on traction power supply and the signaling systems are discussed.

Pantograph Arcing Effects on Traction Power System

The DC component and the extremely low frequency band harmonics can originate from pantograph arcing and cause a problem related to transformer saturation. As it is discussed in [1], the severity of the transformer saturation depends on these currents owing into the circuit, which

in turn depend on the configuration of the traction power system and grounding techniques. This is similar to the effect of geomagnetic induced current, which can also induce DC and extremely low frequency band current into the traction power network. This results in many interference issues and hazards.

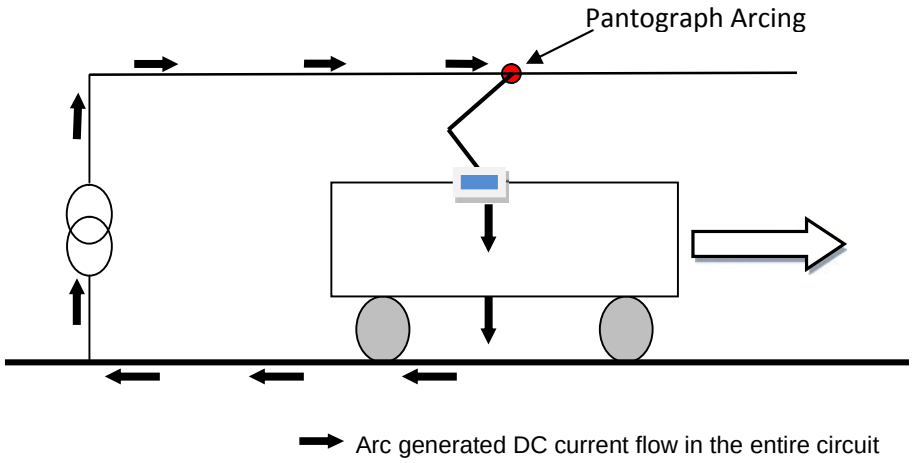

Figure 3.8: DC current generated by the pantograph arcing and its propagation

The leaking impedance between the rail and the earth is finite and since the rails have a longitudinal resistance, a portion of return DC current flows back to the substation through the earth. The return current gets attached to any metal objects (pipelines, fencings, cable shields etc.) running parallel to the rails and returns to the rails/metallic earthing near the substations. Hence an accessible voltage can exist between the running rails and other metallic parts of the traction system. These currents can spread within the entire traction power system affecting the transformers.

Pantograph Arcing Effects on Signaling System

The interference caused by the pantograph arcing can reduce the operational reliability of the functioning of the signaling equipments such as track circuit. The track circuit relay coil has to be energized for a green signal and de-energized to make a red signal. If it is somehow de-energized because of interference current, it will lead to false un-occupancy and vice versa. However to cause interference which may trigger false signaling with the track circuit, the signal characteristics should be identical which is quite uncommon because of different signal processing techniques used in track circuits (modulations techniques coding/decoding etc.).

False occupancy can lead to reduced reliability, service interruption and delay in operation. On the other hand, false un-occupancy can result in collisions and accidents which could be disastrous.

Pantograph Arcing Effects on Train Service Interruption

High transients, as experienced by different railways can be generated as a result of the degradation of the sliding contact performance, especially during winter. Repetitive transients were noticed because of the increased air gap between the pantograph and the contact wire. These transients can trip breakers in the vehicle as well as traction feeding station, leading to train stoppages and service interruption.

As it is discussed in [1], a case in point is the problems experienced by Appenzeller Bahnen, Switzerland in 2003 while introducing the new models of modern trains. The 1000 V DC fed trains draw higher currents while moving in the upward slope of the mountainous terrains. In winter severe arcing were observed and high transients were tripping the onboard feeding circuit breaker, causing unwanted stoppage of the train.

Pantograph Arcing Effects on the Materials of the Contact

The vehicle dynamics or the presence of imperfections in the contact wire and/or rail tracks can cause a variable air gap between the sliding contact electrodes. This may lead to a visible burning arc and as a consequence both the pantograph and the contact wire can get damaged, which might be severe at higher currents. Arcing typically does more harm to the pantograph carbons than to the contact wire, weakening the surface of the carbon and causing it to be eroded which accelerates the degradation of both the contact strips on the bow and the contact wire resulting in a poor energy quality factor.

3.6 Pantograph Arc Modeling

The flowing of current through the arc channel between the breaker contacts is the normal switching action of the circuit breaker before current interruption. Arc voltage is the voltage across the contacts of the circuit breaker that is caused by the current due to non-zero resistance of the arc channel. Since the arc behaves as a non-linear resistance, both arc voltage and arc current cross the zero-value at the same time instant. If the arc is cooled sufficiently, at the time

the current goes through zero, the circuit breaker can interrupt the current, because the electrical power input into the arc channel is zero. During current interruption, the arc resistance increases from practically zero to almost infinite in microseconds. The transient recovery voltage (TRV) immediately builds up across the circuit breaker contacts after current interruption. As the hot gas mixture in the interrupting chamber does not change to a complete insulating state instantaneously, the arc resistance is finite and a small current can still flow.

Arc models were originally developed for better understanding of the current interruption process in high voltage circuit breakers and to be able to design interrupting chambers. The arc model simulates nonlinear behavior of the circuit breaker arc because of the complexity in physical phenomena of circuit breaker during current interruption [11].

Arc models can be classified in three categories [14]:

- Black box models
- Physical models
- Parameter models

Black-box models are defined as a model where only the relation between input and output signals is described, without considering the underlying physical processes. The model consists of one or two differential equations. The mathematical equations of this model give the relation between the arc conductance and measurable parameters such as arc voltage and arc current.

In ***physical arc models***, the arc is described by the equations of fluid dynamics. This model describes the entire physical processes and actually used for design of breakers. The model obeys the laws of thermodynamics in combination of Maxwell's equations. They consist of a large number of differential equations. Conservation of mass, momentum, and energy are the three important expressions in these models.

Parameter models are a variation on black box models in the sense that more complex functions and tables are used for the essential parameters of the black box models.

A brief description of the derivation of a black-box model equations are found in [14] and will be outlined in this section.

General Arc Equation

The arc conductance is a function of the power supplied to the plasma channel, the power transported from the plasma channel by cooling, radiation and time:

$$g = F(P_{in}, P_{out}, t) = \frac{i_{arc}}{u_{arc}} = \frac{1}{R} \tag{3.12}$$

with

g = the arc conductance

P_{in} = the power supplied to the plasma channel

P_{out} = the power transported from the plasma channel

t = time

i_{arc} = the arc current

u_{arc} = the arc voltage

R = the arc channel resistance

The arc conductance g varies with the supplied power P_{in} and the transported power P_{out} in the plasma channel. The stored energy in the channel is:

$$Q = \int_0^t (P_{in} - P_{out})dt \tag{3.13}$$

and the arc conductance can be written as [14]:

$$g = F(Q) = F\left[\int_0^t (P_{in} - P_{out})dt\right] \tag{3.14}$$

Because we are interested in the change of the arc conductance, Equation (3.14) is differentiated

$$\frac{dg}{dt} = \frac{dF(Q)}{dQ}\frac{dQ}{dt} \tag{3.15}$$

and divided by the arc conductance g

$$\frac{1}{g}\frac{dg}{dt} = \frac{1}{g}\frac{dF(Q)}{dQ}\frac{dQ}{dt} \tag{3.16}$$

Differentiation of Equation (3.13) and the result substituted with Equation (3.14) in Equation (3.16) gives us the *general arc equation*:

$$\frac{d[\ln(g)]}{dt} = \frac{F'(Q)}{F(Q)}\left(P_{in} - P_{out}\right) \tag{3.17}$$

To solve this general arc equation, assumptions have to be made. These assumptions give us the different black box models. The classical black box models are the Cassie model and the Mayr model. Both the Cassie and Mayr equation are a solution of the general arc equation.

The Cassie Model

In 1939, A. M. Cassie assumed that the arc channel has the shape of a cylinder filled with highly ionized gas with a constant temperature *T*, but with a variable diameter. The heat content per unit of volume remains constant and so does the conductance per unit of volume. Because of the cooling by the gas flow (convection), the arc channel diameter varies in diameter, but the temperature and the conductance per unit of volume of the remaining plasma channel are not affected.

With

g_0 = the conductivity per unit of volume

P_0 = the cooling or loss of power per unit of volume

D = the arc channel diameter varying with time

Q_0 = the energy content per unit of volume

$u_0 = (P_0/g_0)^{1/2}$ the static arc voltage

The arc conductance can be written as:

$$g = F(Q) = Dg_o \tag{3.18}$$

And for the energy as a function of time

$$Q = DQ_o \tag{3.19}$$

Combining Equations (3.18) and (3.19) results in

$$g = F(Q) = \frac{Q}{Q_o} g_o \tag{3.20}$$

$$F'(Q) = \frac{g_o}{Q_o} \tag{3.21}$$

The dissipated power per unit of length

$$P_{out} = DP_o = \frac{Q}{Q_o} P_o \tag{3.22}$$

And the power supplied to the plasma channel

$$P_{in} = u_{arc}^2 . g \tag{3.23}$$

Equations (3.20), (3.21), (3.22) and (3.23) substituted in the general arc equation

(Equation (3.17)) gives us the *Cassie equation*

$$\frac{d[\ln(g)]}{dt} = \frac{P_o}{Q_o}\left(\frac{u_{arc}^2}{u_o^2} - 1\right) \tag{3.24}$$

The quotient Q_0/P_0 is called the arc time constant τ and can be calculated from the homogeneous differential Equation (3.24)

$$\frac{d[\ln(g)]}{dt} = -\frac{P_o}{Q_o} \tag{3.25}$$

A solution satisfying homogeneous Equation (3.25) is

$$g = g_o e^{-\frac{t}{\tau}} \tag{3.26}$$

The time constant τ in Equation (5.15) can be interpreted as the arc time constant parameter with which the arc channels diameter changes. The *Cassie model* is well suited for studying the behavior of the arc conductance in the high-current time interval when the plasma temperature is 8000 K or more.

The Mayr Model

The *Mayr model* describes the arc conductance around current zero. Mayr considered the arc channel to be cylindrical with a constant diameter. The arc column loses its energy by radial heat transport, and the temperature of the arc channel varies more or less exponentially with the temperature.

$$g = F(Q) = k\, e^{\frac{Q}{Q_o}} \tag{3.27}$$

The cooling or loss of power of the arc channel is assumed to be constant. Therefore, $P_{out}=P_o$ and $P_{in}=u_{arc}.i_{arc.}$

When this is substituted in the *general arc equation* (3.17), we get

$$\frac{d[\ln(g)]}{dt} = \frac{u_{arc} i_{arc} - P_o}{Q_o} \tag{3.28}$$

At the instant of current zero, the power input $u_{\text{arc}}\, i_{\text{arc}}$ in the arc channel is zero, and the rate of change of the conductance of the arc channel is:

$$\frac{dg}{dt} = -g\frac{P_o}{Q_o} \tag{3.29}$$

This is the homogeneous differential equation of Equation (3.29) and has as a solution

$$g = g_o e^{-\frac{P_o}{Q_o}t} \tag{3.30}$$

In this expression Q_0/P_0 is the time constant τ of the arc cooling without thermal input to the arc channel and is called the *arc time constant*.

The *Mayr model* is suited for modeling of the arc in the vicinity of current zero when the temperature of the plasma is below 8000 K.

Cassie Mayr Model

In 1959, T. E. Browne proposed a composition of the Cassie and Mayr model. The *Browne* model uses a Cassie equation for the high current interval and a Mayr equation for the current zero periods.

Chapter 4

MATHEMATICAL MODELING AND ANALYSIS

4.1 Introduction

In the previous chapter, a brief description of the pantograph-catenary contact system, and the characteristics of electric arc has been presented. Pantograph arcing and its effects had also been discussed. In this chapter, mathematical modeling of pantograph-catenary interaction and conductance during pantograph arcing will be presented. Furthermore, the influence of contact distance and the effect of weather condition are also analysed and discussed.

4.2 Pantograph-Catenary Interaction Modeling

Pantograph-caternary interaction can be modeled based on the working principle of both the pantograph and the caternary. The pantograph mechanism consists of a head assembly and a variable height frame assembly. The frame assembly raises the head assembly into forced contact with the catenary system. The catenary system consists of a contact wire suspended from a catenary wire through an arrangement of droppers.

This interaction between the pantograph and the catenary is due to the uplift force of the pantograph in order to get power for the locomotive. The point at the collector strip contacting the overhead contact line couples the two systems. A simple model represents the pantograph by substitute masses which are coupled to one another through springs and dampers. The oscillation behavior of such systems is described by a system of second-order differential equations. The number of equations is determined by the number of substitute masses i.e. the number of degree of freedom of the system. The dynamic model of pantograph-catenary interaction is presented in figure 3.5.

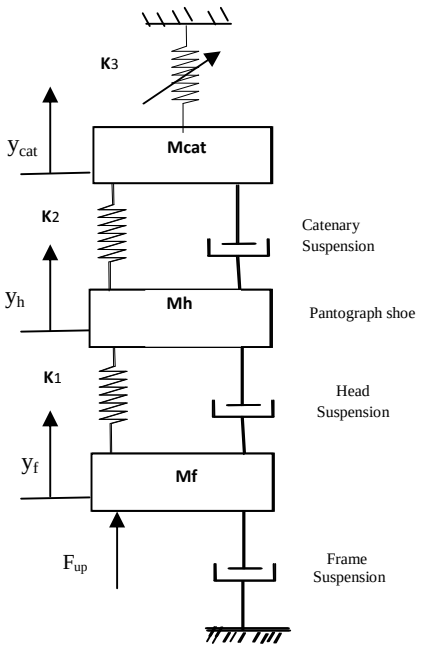

Figure 4.1: The dynamic model of pantograph-catenary interaction

The equation of motion can be written as:

$$\left.\begin{aligned} &m_f \ddot{y}_f + C_f \dot{y}_f + C_h(\dot{y}_f - \dot{y}_h) + k_1(y_f - y_h) = F_{up} \\ &m_h \ddot{y}_h + C_h(\dot{y}_h - \dot{y}_f) + C_{cat}(\dot{y}_h - \dot{y}_{cat}) + k_1(y_h - y_f) + k_2(y_h - y_{cat}) = 0 \\ &m_{cat} \ddot{y}_{cat} + C_{cat}(\dot{y}_{cat} - \dot{y}_h) + k_3 y_{cat} + k_2(y_{cat} - y_h) = 0 \end{aligned}\right\} \quad (4.1)$$

Where:

C_{cat}, C_f and C_h be the damping coefficients of the catenary, frame and head suspensions

y_h, y_f and y_{cat} be the displacement made by head mass, frame mass and catenary

k_3, k_2, k_1 be the stiffness coefficients of the catenary, the head mass and frame mass

Writing equation 4.1 in the Laplace Transformation,

$$\left.\begin{aligned} &\left(m_f s^2 + (C_f + C_h)s + k_1\right)Y_f(s) - (C_h s + k_1)\, Y_h(s) = F_{up} \\ &-(C_h s + k_1)Y_f(s) + (m_h s^2 + (C_h + C_{cat})s + (k_1 + k_2))Y_h(s) - (C_{cat} s + k_2)Y_{cat}(s) = 0 \\ &-(C_{cat} s + k_2)Y_h(s) + (m_{cat} s^2 + C_{cat} s + (k_3 + k_2))Y_{cat}(s) = 0 \end{aligned}\right\} \quad (4.2)$$

The matrix form of equation 4.2 is:

$$\begin{bmatrix} m_f s^2 + (C_f + C_h)s + k_1 & -(C_h s + k_1) & 0 \\ -(C_h s + k_1) & m_h s^2 + (C_h + C_{cat})s + (k_1 + k_2) & -(C_{cat} s + k_2) \\ 0 & -(C_{cat} s + k_2) & m_{cat} s^2 + C_{cat} s + (k_3 + k_2) \end{bmatrix} \begin{bmatrix} Y_f(s) \\ Y_h(s) \\ Y_{cat}(s) \end{bmatrix} = \begin{bmatrix} F_{up} \\ 0 \\ 0 \end{bmatrix} \quad (4.3)$$

From LRT data [7], important data used for solve the matrix in equation 4.3 are stated in Table 4.1 below. The damping coefficient of the catenary (k_3) and stiffness coefficient of the catenary (C_{cat}) will be calculated based on these data.

Table 4.1 : LRT data used for calculation purpose

S.N.	Items	Symbol	Data Value
1	mass of pantograph frame	m_f	12 kg
2	mass of pantograph head	m_h	7 kg
3	mass of contact wire	m'_{CW}	1.35 kg/m
4	mass of catenary wire	m'_{CA}	1.342kg/m
5	tensile force of the contact wire	T_{CW}	12kN
6	stiffness coefficient of pantograph frame	k_1	2650 N/m
7	stiffness coefficient of pantograph head	k_2	10 kN/m
8	damping coefficient of pantograph frame	C_f	70 N.s/m
9	damping coefficient of pantograph head	C_h	0 N.s/m
10	Force exerted by the pantograph	F_{up}	70 N

But, the stiffness of the catenary, k_3, can be calculated as:

$$k_3 = \frac{F}{y_{cat}} = \frac{F}{F.e} = \frac{1}{e} \quad (4.4)$$

Where: F is the contact force and e is the elasticity of the contact wire.

And the elasticity of the contact wire can be calculated as:

$$e = l / \left[k' . (T_{CW} + T_{CA}) \right]$$

The value of k' =4 for the non-stitched catenary and k'=3.5 for stitched catenary [15]. Hence, k'=4 is taken since OCS of AA-LRT is a simple catenary system. The tensile force for both contact and catenary wires is 12kN.

The span length of the catenary suspension of AA-LRT is in the range 30m to 50m based on the radius of curvature of the line.

So, elasticity of at the middle of a span of length 50m is:

$$e = \frac{50m}{4*2*12kN} = 0.52mm/N = 0.00052m/N$$

As it is described in [15], the elasticity at the supports is only 30% to 50% of the mid span value. Take, the elasticity at the supports will be 50% of that of the mid span, i.e. 0.00026m/N.

$$k_{\max} = \frac{1}{e} = \frac{1}{0.00026} = 3846N/m \;\; and \;\; k_{\min} = \frac{1}{e} = \frac{1}{0.00052} = 1923N/m$$

Hence the average stiffness of the catenary will be:

$$k_3 = k_{ave} = \frac{k_{\max} + k_{\min}}{2} = 2884.5N/m$$

Calculating the the damping constant C_{cat}

It is observed from AA-LRT data, the uplift force due to the pantograph is 70N and the mass per unit length of the contact wire, m_{CW} and the catenary wire, m_{CA} is 1.35 kg/m and 1.342 kg/m respectively. The catenary structure is the wiring arrangement of the contact wire, the catenary wire and the dropper in the overhead contact system. In this arrangement, two wires are used for the catenary and contact wire. The structural mass of the catenary system, *m'* (leaving the mass of the dropper) is equal to 2*1.35 + 2*1.342=5.384 kg/m. Then, mass, m of the catenary for 50m span length will be 269.2 kg.

The wave propagation speed can be calculated as:

$$c_w = \sqrt{\frac{T_{CW}}{m'_{CW}}} = \sqrt{\frac{12000}{1.35}} = 94.28 m/s$$

And the first natural frequency will be:

$$f_1 = \frac{c_w}{2l} = \frac{94.28}{2*50} = 0.9428Hz$$

Hence, the angular frequency, ω_1,

$$\mu_1 = 2® f_1 = 5.924 rad/s$$

The frequency range of interest is 0 to 10Hz. Hence, the highest frequency of interest is f_n=9Hz. Therefore, the highest angular frequency, ω_n, will be:

$$\mu_n = 2® f_n = 56.55 rad/\sec$$

The critical damping ratio, ζ , values for wires should between 0.01 and 0.04 [33]. Take ζ =0.04.

$$\sim = , \frac{2\mu_1\mu_n}{\mu_1 + \mu_n} = 0.04\frac{2*5.924*56.55}{5.924+56.55} = 0.429/\sec, and$$
$$= , \frac{2}{\mu_1 + \mu_n} = 0.04\frac{2}{5.924+56.55} = 0.00128\sec$$

From the Rayleigh damping, the damping constant C_{cat} of the catenary structure can be given,

$$C_{cat} = \sim m + \quad k_3 = 119.18 N.s/m$$

Substituting the values in equation 4.3, we have:

$$\begin{bmatrix} 12s^2+70s+2650 & -2650 & 0 \\ -2650 & 7s^2+119.18s+12650 & -119.18s-10000 \\ 0 & -119.18s-10000 & 269.2s^2+119.18s+12884.5 \end{bmatrix} \begin{bmatrix} Y_f(s) \\ Y_h(s) \\ Y_{cat}(s) \end{bmatrix} = \begin{bmatrix} F_{up} \\ 0 \\ 0 \end{bmatrix} \quad (4.5)$$

⇒

$$Y_{cat}(s) = \frac{977.67s^2 + 164{,}066.37s + 6{,}883{,}133.47}{s(s^7 + 115.54s^6 + 4{,}977.7s^5 + 225{,}427.97s^4 + 2{,}922{,}484.7s^3 + 31{,}092{,}036.13s^2 + 46{,}494{,}075.75s + 283{,}634{,}264.37)} \quad (4.6)$$

Thus, the poles of the expression $Y_{cat}(s)$ in equation 4.6 are 0, -83.91, -16.98 ± j39, 5.63 ± j12.38, and 0.36 ± j3.16. And then equation 4.6 can be rewritten as:

$$Y_{cat}(s) = \frac{977.67\,s^2 + 164{,}066.37\,s + 6{,}883{,}133.47}{s(s+83.91)\left(s^2+33.96s+1809.4\right)\left(s^2+11.25s+184.92\right)\left(s^2+0.71s+10.1\right)} \quad (4.7)$$

In order to express equation 4.7 in the time domain form, the value of the constants (K_1,K_2,K_3,K_3^*,K_4,K_4^*, and K5) in equation 4.8 shall be calculated.

$$Y_{cat}(s) = \frac{K_1}{s} + \frac{K_2}{s+83.91} + \frac{K_3}{s+(16.98-j39)} + \frac{K_3^*}{s+(16.98+j39)} + \frac{K_4}{s+(5.63-j12.38)} + \frac{K_4^*}{s+(5.63+j12.38)} + \frac{K_5}{s+(0.36-j3.16)} + \frac{K_5^*}{s+(0.36+j3.16)} \quad (4.8)$$

The values of the constants K_1,K_2,K_3,K_3*,K_4,K_4*, and K_5 are 0.0243, 0,0,0,0.0006 (1-j), 0.0006(1+j), -0.0127-j0.0026, and -0.0127+j0.0026 respectively. Finally, equation 4.6 can be written in the time domain as:

$$y_{cat}(t) = 0.017.e^{-5.63t}.\cos(12.38t + 0.785) + 0.026.e^{-0.36t}.\cos(3.16t + 0.202) + 0.024u(t) \quad (4.9)$$

This expression in equation 4.9 describes the relation between the displacement of the catenary due to the pantograph and the time after the contact.

4.3 Conductance during Pantograph Arcing

As observed from AA-LRT data, the possible train spacing in the common section of the two lines is about 2.16 km. The following table shows the feeding points and the distance between two feeding points along East-West line of AA-LRT.

From table 4.2 below, it is observed that the maximum possible distance between adjacent TPLS is 2.34 km. That means, one TPLS can feed power to the train for half of 2.34 km i.e. for 1.17 km only. Hence, a rectifier substation will not have a possibility to feed two trains at the same time.

Table 4.2: The location of rectifier substations along East-West line of AA-LRT

TPLS	Chain age of feeding point on OCS	Distance b/n two feeding points (km)
EW22 TPLS	YDK5+495.5	
EW20 TPLS	YDK7+116	2.02
	YDK7+516	0.40
EW16 TPLS	YDK9+614.5	2.10
	YDK10+019	0.40
EW13 TPLS	YDK11+507	1.49
	YDK11+705	0.20
EW10 TPLS	YDK13+447	1.74
	YDK13+655	0.21
EW7 TPLS	YDK15+969.84	2.31
	YDK16+177.84	0.21
EW5 TPLS	YCK18+369.019	2.19
	YCK18+577.019	0.21
EW2 TPLS	YCK20+919.019	2.34
	YCK21+127.019	0.21
EW1 TPLS	YCK22+458.5	1.33

Consider that the pantograph losses its contact at a distance x from the substation. The resistance of the contact wire per unit length can be calculated as:

$$R_1 = \frac{^\circ}{A} = \frac{1.777*10^{-2}}{150} = 1.185*10^{-4}\,\Omega/m = 1.185*10^{-7}\,\Omega/mm$$

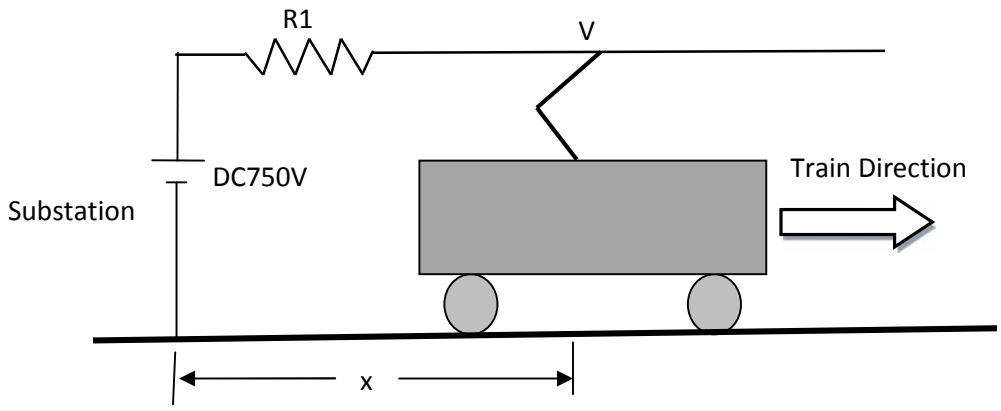

Figure 4.2: The rectangular loop model of a train movement

As it is observed from AA-LRT data, the maximum possible current *I* drawn by the train is 210A. The arc voltage V_{arc} at the point of the pantograph losses the contact can be calculated as:

$$V_{arc} = 750 - R_1 I\, x = 750 - 0.024885x;\ \ for\ \ 0 \le x \le 1.17 km \qquad (4.10)$$

From equation (4.10), it can be seen that the arc voltage decreases as the increase of the distance of the pantograph from the substation.

The initial arc conductance, g_o, can be calculated as:

$$g_o = \frac{I}{V_{arc}} = \frac{210}{750 - 0.024885x} \qquad (4.11)$$

As it is seen in equation (4.11), g_o value will increases from 0.280 Siemens to 0.291 Siemens as x increases to 1170m.

From Mayrs electric arc model, we have:

$$\frac{1}{g}\frac{dg}{dt} = \frac{1}{\tau}\left(\frac{ui}{P} - 1\right)$$

At the instant of current zero, the power input is zero and therefore, *ui=0*. Then the above equation is to be:

$$\frac{dg}{dt} = -g_o . \frac{1}{\tau}$$

which is homogenous differential equation with solution:

$$g = g_o . e^{-\frac{1}{\tau}t}$$

But substituting equation (4.11), we have:

$$g = \left(\frac{210}{750 - 0.024885\, x}\right) . e^{-\frac{1}{\tau}t} \qquad (4.12)$$

4.4 The Influence of Contact Distance

Whenever the pantograph strip losses its contact with the contact wire, electric field in the air gap is produced. That means, when air molecules become ionized in a very high electric field, the air will change from an insulator to a conductor. Sparks occur because of the recombination of electrons and ions. Then the continuous discharge phenomenon takes place.

Paschen's Law states that the breakdown voltage of a uniform field gap in a gas is the relation of the voltage to the product of the gas pressure times the gap length. In general, this law can be written as:

$$V_B = f(pd) \tag{4.13}$$

Where p is the gas pressure and d is the distance between parallel plates. This equation gives the breakdown voltage that is the voltage necessary to start a discharge or electric arc. The empirical formula to find the breakdown voltage is [19]:

$$V_B = \frac{apd}{\ln(pd)+b} \tag{4.14}$$

Where V_B is the breakdown voltage in Volts, p is the pressure in Atmospheres or bar, and d is the gap distance in meters. The constants a and b depend upon the composition of the gas. For air at standard atmospheric pressure of 101 kPa = 1 atm, $a = 4.36\times10^7$ *V/(atm·m) and* $b = 12.8$[19].

In order to calculate the minimum breakdown voltage, first differentiate the above equation with respect to pd and then setting the derivative to zero.

$$\frac{dV_B}{d(pd)} = \frac{d}{d(pd)}\left(\frac{apd}{\ln(pd)+b}\right)$$

$$\frac{dV_B}{d(pd)} = \frac{a(\ln(pd)+b-1)}{(\ln(pd)+b)^2} = 0 \tag{4.15}$$

Hence, $pd = e^{1-b}$. By taking $p=1$ *atm*, $d=7.5\mu m$. And then the minimum breakdown voltage will be about 327V. For air at STP, the voltage needed to arc a 7.5µm gap is about 327V. The intensity of the electric field for this gap is therefore 43.6MV/m.

Just at the beginning of a disconnection, the gap between the pantograph and catenary is small, so it is easy to break down, which causes gap discharges and arc generation. With the increasing spacing, the arc is stretched. Energy which is absorbed by the arc cannot support the arc continuing burning, so the arc will be extinguished and the pantograph separates completely from the contact wires.

Since the electrical conductivity of air is very low, air is an excellent insulator. The dielectric strength of air is 3kV/mm, which means that is two electrodes are placed one millimeter away from each other in air, then the air normally acts as an insulator until the voltage between the electrodes reaches 3kV or 3000V, after which the air starts behaving as a good conductor which causes sparks and fire [20].

The separation *d* depends on the arc voltage, i.e. as the arc voltage increases, the possible separation of the contact that produces an arc increases also. From equation 4.10, the electric field strength *E* which can produce arc in the medium air, can be written as:

$$E = \frac{V_{arc}}{d} = \frac{750 - 0.024885.x}{d}$$

The arc voltage at instant the vehicle around the substation is about 750V and air is the insulating medium between the contact wire and the pantograph strip. In order to produce a pantograph arcing in the operation of AA-LRT, the maximum possible separation *d* of the pantograph strip from the contact will be:

$$d = \frac{750V}{3kV/mm} = 250\mu m = 0.25mm$$

Pantograph arcing will produce if the separation between the pantograph and the contact wire is less than 0.25mm. That means, the electric field produced due to the separation will become zero at the distance 0.25mm from the contact wire. If it is 0.25mm and greater, no arcing but power interruption will be occurred.

4.5 The Influence of Weather Condition

The weather condition of the environment is the other factors that influence on the production of pantograph arcing in railway system. A layer of ice/snow is also formed on the contact wire which depends on the meteorology conditions. The icing on the overhead contact wire could be formed mainly from two sources [1]:

a) Fog: - As the temperature decreases, the air get saturated by the moisture content and condensation starts. This can lead to a water/moisture layer on the overhead conductor. As the temperature falls below zero, this water layer and small droplets of water present in the atmosphere on the contact wire freeze and cause a layer of ice to accumulate on it.

b) Precipitation: - Rains and snowflakes can precipitate on the contact wire and form an ice layer.

The fluctuations in temperature between day and night, sometimes formed and concentrated a solid ice layer at the bottom of the contact wire where the pantograph makes contact. This made the situation even worse. They cause a clearly visible pantograph arcing moving with the pantograph along the contact wire. This in turn degrades the life and performance of both the contact wire and the pantograph, causing interference problems.

The current collection performance by the pantograph is influenced by the characteristics of the ice layer, i.e., hardness, surface smoothness, sticking tendency etc. when the pantograph moving through ice layered contact wire. Common belief in the railway community is that the ice can be easily scrapped using a scrapping pantograph. However it has been shown that even after two pantographs passed through a line, the scrapping of the overhead contact wire was not complete. Intense arcing was noticed when another train passes through the same track [1].

As it is reported by World Weather taking the data from year 2000 to 2012, the lowest average low temperature of Addis Ababa is 6^{o}C (on the months of November and December) and its average temperature is 25^{o}C (on the months of March, April and May). On the other hand, the monthly the highest average rainfall amount is 189 mm which is on the month of August. It is known that water freezes to ice when the temperature is 0^{o}C and below it. Hence, the weather condition of Addis Ababa is not as such that to make an accumulation of ice on the contact wire even in the worst condition. The rain leaves water/moisture layer on the contact wire will be have a chance to convert to ice due to the temperature of Addis Ababa. Therefore, the weather condition can not be the cause of pantograph arcing for AA-LRT.

Chapter 5

SIMULATION RESULTS AND DISCUSSION

5.1 Introduction

In the previous chapters, the mathematical modeling of the pantograph-catenary interaction system and the conductance during pantograph arcing have been discussed. The influence of some parameters like contact distance and the weather condition have been also analyzed and discussed in detail in chapter 4. In this chapter, the MATLAB simulation results of the influential parameters of pantograph arcing using the mathematical modeling discussed in chapter 4 and discussions on the results found from the simulation are presented.

5.2 Simulation Result of the Influence of Vibration of the Catenary System

The uplift of the contact wire gets bigger and the contact between the pantograph and the catenary is harder to maintain due to increase in the amplitude of the catenary oscillations. In order to avoid this deterioration of the contact quality the train speed should not exceed 70-80% of the contact wire wave propagation speed [4]. For the train having two pantographs, it will have a sufficient distance between the two pantographs in order to keep the rear pantograph influenced by the mechanical oscillation due to the contact force of the front pantograph. However, arcing on the rear pantograph is commonly noticeable.

When a pantograph pushes up the contact wire at a point, the contact wire form a wave which oscillates and takes some time to be damped after the pantograph has gone. In this section, it is going to be simulated the waveform of vibration of the contact wire so as to determine the minimum distance between two consecutive pantographs which is used to avoid the occurrence of arcing on the trailing pantograph due to the contact loss caused by the wave produced by the first pantograph.

As it is already discussed in the previous chapter, the damping constant of the catenary, C_{cat} and the stiffness coefficient of the the catenary, k_3 are parameters that determine the intensity of vibration of the contact wire. These parameters are by themselves dependent on the span length of the OCS and the weight of the catenary. Hence, in this section, the effect of the vibration

made by the pantograph with span length of 20, 30 and 50 meters and the weight of the catenary is taken under consideration. Below the simulation results of these effect is presented based on the calculations and the inputs made in the previous chapter. Figure 5.1(a), 5.2(a) and 5.3(a) are the simulation results using the present (full) weight of the catenary as the whole whereas figure 5.1(b), 5.2(b) and 5.3(b) are the simulation results taking half of the weight of the present weight of the catenary.

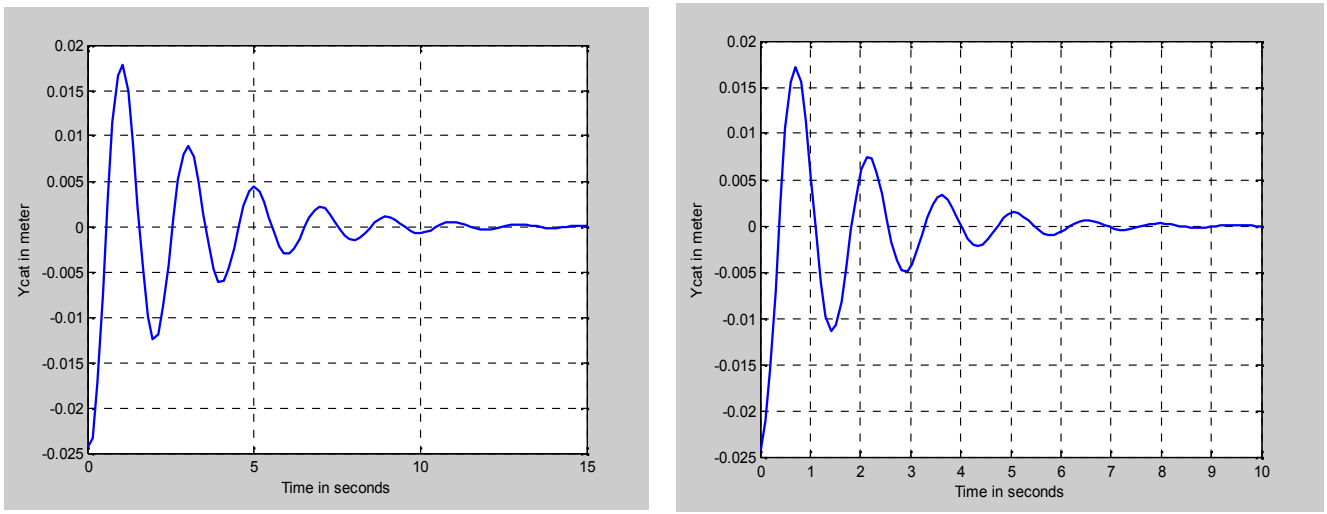

(a) *(b)*

Figure 5.1: The waveform of the vibration of the AA-LRT catenary structure for 50m span length

Figure 5.1(a) above shows the waveform of the vibration of the catenary structure of 50m span length after the contact force leaves the point of contact for the case of AA-LRT. From this, it is observed that the oscillation of the wire stays only about 12 seconds after the force removed at the point of contact. Hence, the distance covered by the train with the maximum operational speed of 50km/h for 12 seconds will be 167 meters. But, from figure 5.1(b), the vibration of the catenary stays only 7 seconds.

Similarly, figure 5.2(a) above shows the waveform of the vibration of the catenary structure of 30m span length after the contact force leaves the point of contact for the case of AA-LRT. From this, it is observed that the oscillation of the wire stays only about 7 seconds after the force removed at the point of contact. Hence, the distance covered by the train with the maximum operational speed of 50km/h for 7 seconds will be 97 meters. But, from figure 5.2(b), the vibration of the catenary stays only 3 seconds.

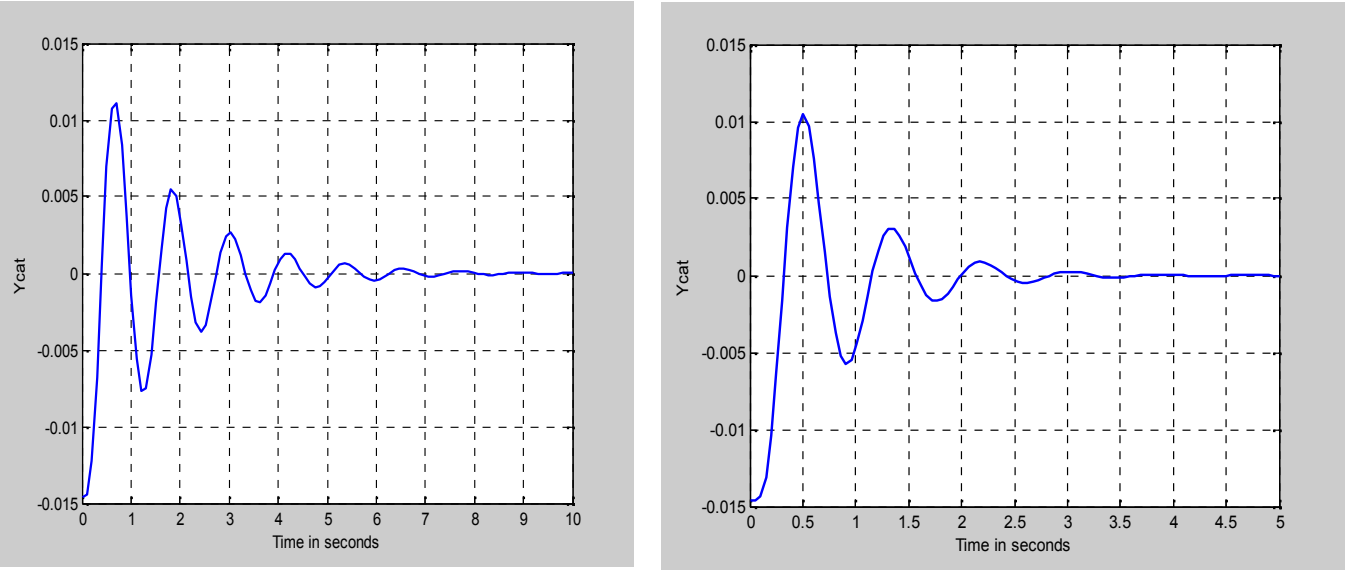

(a) *(b)*

Figure 5.2: The waveform of the vibration of the AA-LRT catenary structure for 30m span length

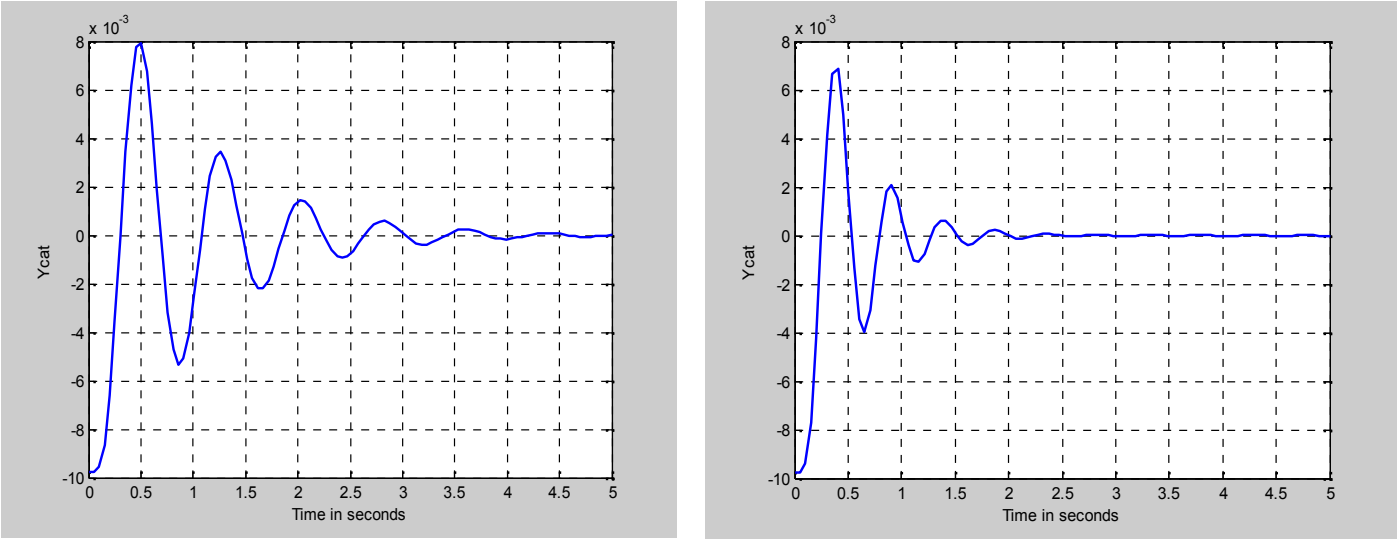

(a) (b)

Figure 5.3: The waveform of the vibration of the AA-LRT catenary structure for 20m span length

As it is also observed Figure 5.3 that the waveforms of the vibration of the catenary structure of 20m span length after the contact force leaves the point of contact for the case of AA-LRT. From this, it is observed that the oscillation of the wire sustains within 4 seconds after the force

removed at the point of contact. Whereas, the vibration sustains within 2 seconds if half of the catenary weight is used.

The above simulation results are made by taking parameters the weight of the catenary (the weight of the catenary of AA-LRT as the whole and its half weight) and the span length of the OCS (20m, 30m, and 50m). In order to put the conclusion of the section, the important results are summarized in Table 5.1 below.

Table 5.1: Summary of simulation result

S.N.	Span Length (meter)	Weight of Catenary (Half, Full)	Time Taken by the Catenary Vibration (second)	Minimum Distance between the Pantographs (meter)
1	50	Full	12	167
		Half	7	97
2	30	Full	7	97
		Half	3	42
3	20	Full	4	56
		Half	2	28

From Table 5.1, the decreasing of the weight of the catenary and/or the span length of the OCS can decrease the time of the vibration of the catenary. As the result, it decreases the minimum distance between the pantographs in operation so as to avoid the contact loss due to the vibration. The weight of the catenary end the span length of the OCS are the influential parameters for pantograph arcing.

5.3 Simulation Result of Conductance during Pantograph Arcing

Whenever the pantograph strip losses its contact with the contact wire, electric field in the air gap is produced. That means, when air molecules become ionized in a very high electric field, the air will change from an insulator to a conductor and electric current will flow through it.

From equation 4.12, it can be seen that the arc conductance depends on the arc time and the distance x from the substation pantograph arcing happens. As it is observed from figure 5.4, the voltage will drop from 750V to 720V as the train travels about 1.2km away from the substation.

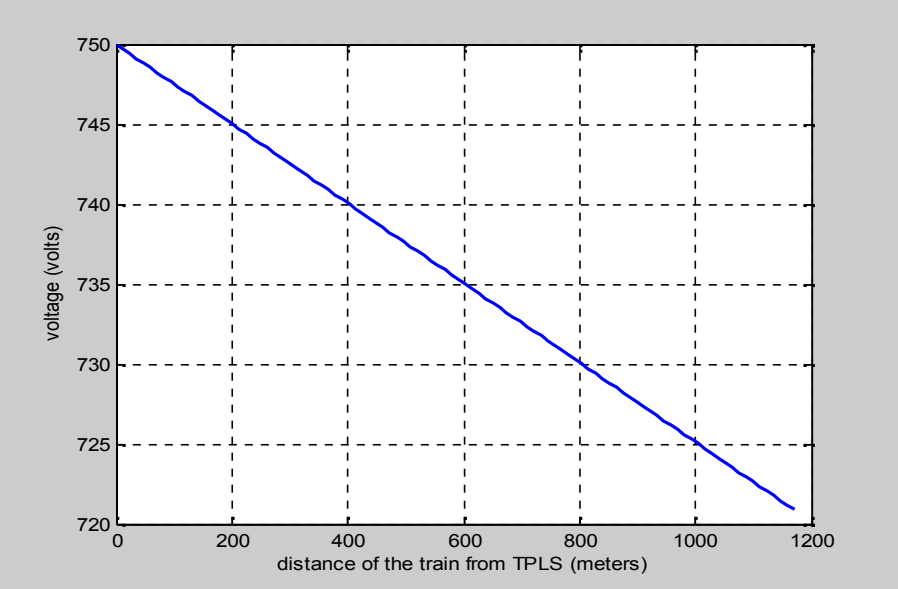

Figure 5.4: The relationship between voltage and distance of the train from TPLS

As it is indicated in [28], arc time constant value is in the order of10^{-6} to10^{-3} s, the lower limit typical in HV circuit breakers, whereas the higher one in air at atmospheric pressure. Hence, we take the arc time constant 1ms for the pantograph arcing case.

The following graph shows how the arc conductance decreases through time.

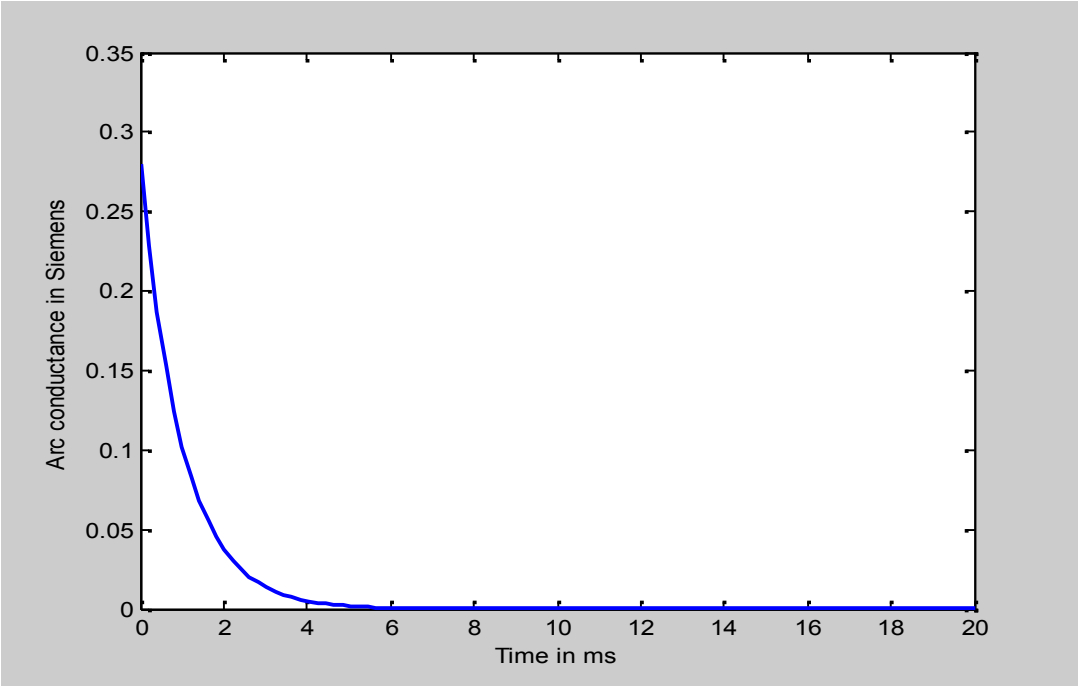

Figure 5.5: The relation between arc conductance and time

As it is observed from figure 5.5 above, the arc conductance decreases at high rate and losses its conductivity within 6 milliseconds of time after the pantograph losses its contact. As the result, although pantograph arcing occurs in the operation of AA-LRT, it will disappear soon.

5.4 Simulation Result of the Influence of Contact Force and Speed of the Pantograph

There are different parameters that influences on pantograph arcing. In this subsection, the influence of contact force and speed of the pantograph is presented.

The contact force of the pantograph is a vertical force exerted by the pantograph so as to collect power from the overhead contact system to the locomotive. The proper balance between the dynamic characteristics of the pantograph and the contact line depends on the quality of current collectors and on the longevity of the contact wire. The pantograph must support them with sufficient force to remain in permanent contact with the wire.

As it is observed from AA-LRT data, the AA-LRT vehicle uses CED-125D type of pantograph. This pantograph is used for the speed up to 120km/h and it is prepared for train operates in the DC1500V overhead contact system. The possible range of contact force applicable for this pantograph is 60N to 140N. As it is observed in [7], 60N is the static force which is the force exerted to the contact wire whenever the vehicle is at stand still or with zero speed. As it is discussed in [15], the uplift coefficient of the pantograph is 0.00228. Hence, from equation 3.1, the mean contact force is the sum of the static contact force and the aerodynamic contact force which is the force due to the dynamic effect of the train, i.e.

$$F_m = 0.00228.v^2 + 60\,(N) \tag{5.1}$$

Where v is the speed of the train in km/h.

As it is observed in equation 5.1, the mean contact force depends on the speed of the pantograph. This implies that as the contact force should be increase with the speed of the pantograph. As it is shown in figure 5.6, the relationship between the contact force and the speed of the train is upward parabolic type. However, the data obtained from the AA-LRT, the operation is made using the same contact force, 70N, for any speed of the train.

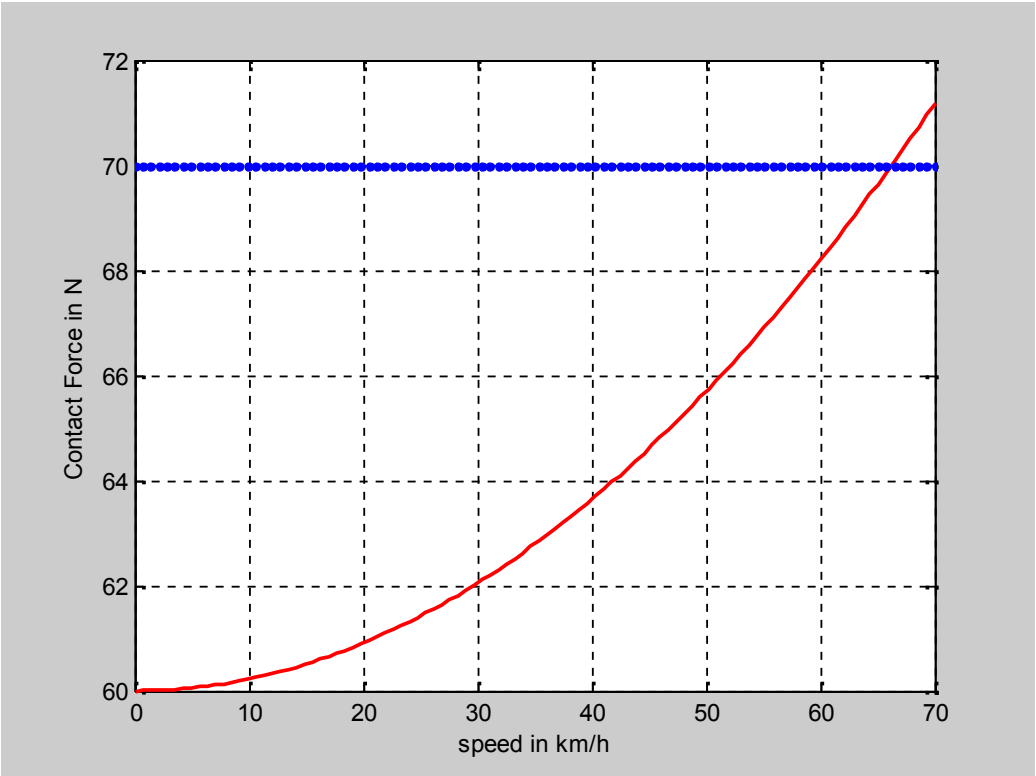

Figure 5.6: The relationship between the contact force and speed

As it is read from the graph in figure 5.6, the force required to raise the contact wire whenever the train is at zero speed or at standstill is 60N and then the contact force increases as the speed increases. Whenever the speed reaches to about 65km/h, the contact force will be 70N. Up to 65 km/h, the required contact force is less than 70N. So, contact loss will not occur if the speed of the train is less than or equal to 65km/h. If the speed is greater than 65 km/h, the force required to raise the contact wire will be greater than 70N. This implies there will be a contact loss if the speed is greater than 65km/h. However, the maximum operational speed of the train for the case of AA-LRT is less than this speed. Hence, the contact loss will not be occurred in the operation of AA-LRT due to the increase of the speed.

Chapter 6

CONCLUSIONS, RECOMMENDATIONS AND FUTURE WORK

6.1 Conclusions

In order to make the electric traction train move from one place to another, electric power has to be supplied to it. The main objective of the traction power supply is to ensure uninterrupted, reliable and safe operation of the electric traction train. The sliding contact between pantograph and overhead line is a critical interface between the train and high voltage supply in an electrified railway.

Pantograph arcing is the commonly observed phenomenon which can be caused by the loss of contact of the pantograph and the contact wire due to different reasons. Some of the causes of pantograph arcing are contact distance, contact force, train speed and the accumulation of ice on the contact wire. The most important and descriptive measurement for the performance of the catenary–pantograph system is the contact force. Too low contact force results in arcing between the contact wire and pantograph, which results in increased wear of the system and could lead to loss of power. If the contact force is too high, unacceptable wear of the contact wire and pantograph will occur. Moreover, the vibration of the contact wire after the force leaves is the other cause that produces the loss of contact of the pantograph and the contact wire. Large vertical displacements of the contact wire could occur if contact force is too high, which would have negative effects on a trailing pantograph in the case of trains that have more than one.

Since a pantograph arcing has no its own developed model due to its dynamic characteristics, arc models developed for better understanding of the current interruption process in high voltage circuit breakers was adopted and examined in this thesis. During arcing, the air gap will be ionized and the breakdown voltage produced in it develops its arc conductivity property. However, its conductivity will not stay a long time rather diminishes within a few seconds after the current interrupted from the source.

It has been clearly seen that the vibration of the catenary system due to the passing pantograph is one of the parameters that affect the occurrence of pantograph arcing for the case of AA-LRT. The span length of the OCS and the weight of its catenary are factors that contribute for the

contact loss between the contact wire and the pantograph strip. The result found in this regard that the minimum distance between the two vehicles shall not be less than 167 meters so as to avoid the contact loss on the following pantograph due to the vibration produced by the front one. Since the distance between the front and the rear pantograph in coupled LRT vehicle is only 30 meters, the vibration produced by the front pantograph can cause contact loss for the rear pantograph. From this study, it can be observed that AA-LRT needs to reduce its span length to 20m and also the weight of the catenary to half in order to introduce coupled vehicles in operation.

Pantograph arcing will produce if the separation between the pantograph and the contact wire is less than 0.25mm. That means, the electric field produced due to the separation will become zero at the distance 0.25mm from the contact wire. In addition to this, this arcing will be disappeared within six milliseconds of its occurrence.

Even though weather condition and speed of the train are the main parameters for pantograph arcing, they are not a problem for the operation of AA-LRT.

6.2 Recommendations

The purpose of this thesis is to study the pantograph arcing and the parameters that cause it for the case of AA-LRT. Some of the parameters that cause the occurrences of pantograph arcing are the pantograph contact force, the vibration of the contact wire, the laying of ice/water on the contact wire, and the separation distance of the pantograph strip and the contact wire. Based on the results of the study, the following are options of recommendations for the railway operator company which will be engaged in the AA-LRT operation in order to reduce the occurrence of pantograph arcing.

i) Whenever the railway operating with the coupled Light rail vehicle, it should reduce the length of the span to 20 meters and also reduce the catenary weight to half. This will expose to a bit change of the railway infrastructure and also the specification which needs a lot of budget.

ii) Whenever the railway operating with the uncoupled Light rail vehicle, it should keep the distance between the vehicles in operation to the minimum 167 meters.

Hence, the railway operating company is recommended to give service with uncoupled rail transit vehicle keeping the distance between the two vehicles is greater than 167 meters.

6.3 Suggestions for Future Work

Pantograph arcing is the major source of electromagnetic interference (EMI). It can distort the waveform of the supply voltage and current, generates transients and can interference with the traction power and the signaling system in electrified railways.

This thesis only focuses on the investigation of the influential parameters of the pantograph arcing for the case study on AA-LRT and then recommended the mitigation measures for the occurrence of pantograph arcing. Studying the cause and effects of pantograph arcing for Addis Ababa-Djibouti railway operation, which has 25kV, 50Hz AC traction power supply, is my suggestion for the future work.

REFERENCES

[1] Surajit Midya, "Conducted and Radiated Electromagnetic Interference in Modern Electrfied Railways with Emphasis on Pantograph Arcing", Doctoral Thesis in Electrical Systems, Stockholm, Sweden, 2009

[2] Pierre-vincent Verschraegen, "A Model of the Pantograph Arc Impedance for 50 Hz Catenary Voltage", Master of Science Thesis, Stockholm, Sweden, 2010.

[3] Mustafa Karagoz, "Analysis of the Pantograph Arcing and its effects on the Railway Vehicle", Master of Science Thesis, Middle East Technical University, January 2014

[4] Pedro Cabaço Antunes, "Development of Multibody Pantograph and Finite Element Catenary Models for Application to High-speed Railway Operations", Instituto Superior Técnico – Universidade Técnica de Lisboa

[5] Jin Wang, Zhongping Yang, Fei Lin and Junci Cao, "Harmonic Loss Analysis of the Traction Transformer of High-Speed Trains Considering Pantograph-OCS Electrical Contact Properties" School of Electrical Engineering, Beijing Jiaotong University, No. 3 ShangyuanCun, Beijing 100044, China, School of Electrical Engineering, Beijing Jiaotong University, No. 3 ShangyuanCun, Beijing 100044,November 2013

[6] Zhang, Qin, Cheng, Jia, Xing, "An Analysis Method for the Correlation between Catenary Irregularities and Pantograph-catenary Contact Force", State key laboratory of rail traffic control and safety, Beijing Jiaotong University, Beijing, China, 2012

[7] "Technical Specification of Vehicles of AA-LRT phase I Project", China Railway Group Limited, July 2013.

[8] Sheilah Frey, "Railway Electrification System and Engineering", Delhi University, India, 2012

[9] Tiago Manuel Oliveira Valezim Teixeira, "Dynamic and Control of High-speed Train Pantograph System", Technical University of Lisbon, Institute of Engineering Science and Technology, Portugal, September 2007

[10] "Vehicle System Dynamics Supplement", Taylors and Francis, International Journal of Vehicle Mechanics and Mobility

[11] P.h. Schavemaker and L. Van Der Sluis,"The Arc Model Blockset", Delft University of Technology, The Netherlands.

[12] Simon Walters, Ahmed Rachid, Augustin Mpanda, "On Modelling and Control of Pantograph Catenary Systems".

[13] Niklas Gustavsson, "Evaluation and Simulation of Black-box Arc Models for High Voltage Circuit-breakers", Linköping University, Sweden**,** March 2004.

[14] Lou van der Sluis, "Transients in Power Systems", Delft University of Technology, The Netherlands, 2001.

[15] Kiessling, Puschmann, Schmieder, Schneider, "Contact Lines for Electric Railways-Planning, Design, Implementation, Maintenance", 2nd edition, 2009.

[16] Midya, S.; Bormann, D; Larsson, A; Schutte, T; Thottappillil, R; "Understanding pantograph arcing in electrified railways - influence of various parameters", IEEE International Symposium, August 2008, University of Uppsala, Uppsala, Sweden

[17] Esiee Amiens team, "Report on Pantograph - Catenary Dynamics and Physical Phenomena", Pacific Project, October 2011

[18] Michael A. Lieberman and Allan J. Lichtenberg, "Principles of plasma Discharges and materials Processing, 2nd Edition", 2005, USA

[19] "High Voltage Design Guide for Airborne Equipment", Technical Report, Boeing Aircraft Company, June 1976.

[20] Rigden, John S. Macmillan Encyclopedia of Physics, Simon & Schuster, 1996.

[21] Petter Roe Navik, "Numerical Analysis of the Dynamic Behavior of Railway Catenary System in Accoedance with Norwegian Conditions", Master Thesis, Norwegian University of Science and Technology, June 2013.

[22] A. K. Chopra," Dynamics of structures: theory and applications to earthquake engineering", Upper Saddle River, N.J.: Pearson Prentice Hall, 2007.

[23] Xavier Perpiny, '"Infrastructure Design, Signalling and Security in Railway", Janeza Trdine 9, 51000 Rijeka, Croatia, March, 2012

[24] Giorgio Boschetti1, Andrea Mariscotti1, Virginie Deniau2, "Pantograph Arc Transients Occurrence and GSM-R Characteristics", Dept. of Naval and Electrical Eng., Univ. of Genova, Via Opera Pia 11A - 16145 Genova – Italy.

[25] S. Niska, "Railway EMI impact on train operation and Environment", Electrical Power systems, Sweden.

[26] Midya, S.; Bormann, D; Larsson, A; Schutte, T; Thottappillil, R; "Understanding pantograph arcing in electrified railways - influence of various parameters", IEEE International Symposium, August 2008, University of Uppsala, Uppsala, Sweden

[27] Midya, S.; Bormann, D; Schutte, T; Thottappillil, R; "Pantograph Arcing in Electrified Railways—Mechanism and Influence of Various Parameters—Part I: With DC Traction Power Supply", IEEE Transactions on Power Delivery , 2009; Stockholm, Sweden.

[28] László Koller, Balázs Novák, Ádám Tamus, "Electrical switching devices and insulators", Budapest University of Technology and Economics Department of Electric Power Engineering, Hungary.

[29] Vikramjit Singh, "Examination of Electric Arc Behavior in Open Air", School of Electrical Engineering, Aalto University, 2012, Finland.

[30] M. F. Hoyaux, "Arc Physics", Springer-Verlag, 1968, New York.

[31] Heinz Maecker et al," The electric arc", 2009, Germany.

[32] Bauer, Westfall, "Physics for Scientists and Engineers 1", Published by McGraw Hill, 2008, USA.

[33] Arnar Kári Hallgrímsson, "Dynamic behavior of contact lines for railways with laboratorial model setup according to Norwegian conditions", Norwegian University of Science and Technology, Department of Structural Engineering, 2013, Norway.

[34] Conceptual and schematic design documents of AA-LRT, 2012.

APPENDICES

Appendix A: MATLAB codes for simulation of pattern of contact wire for 50 meters with full weight

```
n=[37.1 7168.7 423807.3 6883133.6]; % coefficient of numerator

d=[1 129.83 6271.79 231733.73 2792864.31 32183724.88 45897701.4
283634264.37 0]; % coefficient of denominator

disp(['Num=' poly2str(n,'s')]);

disp(['Dem=' poly2str(d,'s')]);

[r,p,k]=residue(n,d)

M2=2*abs(r(2))

phi2=angle(r(2))

w2=abs(imag(p(2)))

a2=-real(p(2))

M4=2*abs(r(4))

phi4=angle(r(4))

w4=abs(imag(p(4)))

a4=-real(p(4))

M6=2*abs(r(6))

phi6=angle(r(6))

w6=abs(imag(p(6)))

a6=-real(p(6))

t=linspace(0,15);

f=M2*exp(-a2*t).*cos(w2*t+phi2)+M4*exp(-a4*t).*cos(w4*t+phi4)+M6*exp(-
a6*t).*cos(w6*t+phi6);

plot(t,f,'linewidth',1.5);

xlabel('Time in seconds');

ylabel('Ycat in meter');
```

```
grid on
```

Appendix B: MATLAB codes for simulation of pattern of contact wire for 50 meters with half weight

```
n=[37.8 13390.3 1335976.6 26707858.8];

d=[1 200.47 8445.94 400749.06 4355902.18 60364352.68 23027462.67
1100554505.23 0];

disp(['Num=' poly2str(n,'s')]);

disp(['Dem=' poly2str(d,'s')]);

[r,p,k]=residue(n,d)

M2=2*abs(r(2))

phi2=angle(r(2))

w2=abs(imag(p(2)))

a2=-real(p(2))

M4=2*abs(r(4))

phi4=angle(r(4))

w4=abs(imag(p(4)))

a4=-real(p(4))

M6=2*abs(r(6))

phi6=angle(r(6))

w6=abs(imag(p(6)))

a6=real(p(6))

t=linspace(0,10);

f=M2*exp(-a2*t).*cos(w2*t+phi2)+M4*exp(-a4*t).*cos(w4*t+phi4)+M6*exp(-
a6*t).*cos(w6*t+phi6);

plot(t,f,'linewidth',1.5);

xlabel('Time in seconds');

ylabel('Ycat in meter');

grid on
```

Appendix C: MATLAB codes for simulation of pattern of contact wire for 30 meters with full weight

```
n=[1562.46 273443.95 11963770.96];

d=[1 118.7 5091.04 238003.75 3172365.42 38259916.15 114379346.59
820372866.09 0];

disp(['Num=' poly2str(n,'s')]);

disp(['Dem=' poly2str(d,'s')]);

[r,p,k]=residue(n,d)

M2=2*abs(r(2))

phi2=angle(r(2))

w2=abs(imag(p(2)))

a2=-real(p(2))

M4=2*abs(r(4))

phi4=angle(r(4))

w4=abs(imag(p(4)))

a4=-real(p(4))

M6=2*abs(r(6))

phi6=angle(r(6))

w6=abs(imag(p(6)))

a6=-real(p(6))

t=linspace(0,10);

f=M2*exp(-a2*t).*cos(w2*t+phi2)+M4*exp(-a4*t).*cos(w4*t+phi4)+M6*exp(-
a6*t).*cos(w6*t+phi6);

plot(t,f,'linewidth',1.5);

xlabel('Time in seconds');

ylabel('Ycat');

grid on
```

Appendix D: MATLAB codes for simulation of pattern of contact wire for 30 meters with half weight

```
n=[1640.66 546887.9 45573991.52];

d=[1 190.15 6256.7 421576.46 5695596.2 89203499.3 401783257.47
3125073704.57 0];

disp(['Num=' poly2str(n,'s')]);

disp(['Dem=' poly2str(d,'s')]);

[r,p,k]=residue(n,d)

M2=2*abs(r(2))

phi2=angle(r(2))

w2=abs(imag(p(2)))

a2=-real(p(2))

M4=2*abs(r(4))

phi4=angle(r(4))

w4=abs(imag(p(4)))

a4=-real(p(4))

M6=2*abs(r(6))

phi6=angle(r(6))

w6=abs(imag(p(6)))

a6=-real(p(6))

t=linspace(0,5);

f=M2*exp(-a2*t).*cos(w2*t+phi2)+M4*exp(-a4*t).*cos(w4*t+phi4)+M6*exp(-
a6*t).*cos(w6*t+phi6);

plot(t,f,'linewidth',1.5);

xlabel('Time in seconds');

ylabel('Ycat');

grid on
```

Appendix E: MATLAB codes for simulation of pattern of contact wire for 20 meters with full weight

```
n=[1341.04 410165.92 31363046.62];

d=[1 177.04 6016.22 386969.47 5244666.72 81566504.88 378518077.02
3208681612.95 0];

disp(['Num=' poly2str(n,'s')]);

disp(['Dem=' poly2str(d,'s')]);

[r,p,k]=residue(n,d)

M2=2*abs(r(2))

phi2=angle(r(2))

w2=abs(imag(p(2)))

a2=-real(p(2))

M4=2*abs(r(4))

phi4=angle(r(4))

w4=abs(imag(p(4)))

a4=-real(p(4))

M6=2*abs(r(6))

phi6=angle(r(6))

w6=abs(imag(p(6)))

a6=-real(p(6))

t=linspace(0,5);

f=M2*exp(-a2*t).*cos(w2*t+phi2)+M4*exp(-a4*t).*cos(w4*t+phi4)+M6*exp(-
a6*t).*cos(w6*t+phi6);

plot(t,f,'linewidth',1.5);

xlabel('Time in seconds');

ylabel('Ycat');

grid on
```

Appendix F: MATLAB codes for simulation of pattern of contact wire for 20 meters with half weight

```
n=[1525 820331.85 110318968.19];

d=[1 289.13 7856.35 686459.46 9427375.64 195593253.09 1267752389.98
11286481477.72 0];

disp(['Num=' poly2str(n,'s')]);

disp(['Dem=' poly2str(d,'s')]);

[r,p,k]=residue(n,d)

M2=2*abs(r(2))

phi2=angle(r(2))

w2=abs(imag(p(2)))

a2=-real(p(2))

M4=2*abs(r(4))

phi4=angle(r(4))

w4=abs(imag(p(4)))

a4=-real(p(4))

M6=2*abs(r(6))

phi6=angle(r(6))

w6=abs(imag(p(6)))

a6=-real(p(6))

t=linspace(0,5);

f=M2*exp(-a2*t).*cos(w2*t+phi2)+M4*exp(-a4*t).*cos(w4*t+phi4)+M6*exp(-
a6*t).*cos(w6*t+phi6);

plot(t,f,'linewidth',1.5);

xlabel('Time in seconds');

ylabel('Ycat');

grid on
```

Appendix G: MATLAB codes for simulation of the relation between arc conductance and time

```
t=linspace(0,20);

xo=1170;

go=(210/(750-0.024885*x0));

g=go.*exp(-t);

plot(t, g,'blue','linewidth',1.5)%,,t,g3,'green')

xlabel('Time in ms')

ylabel('Arc conductance in Siemens')
```

Appendix H: MATLAB codes for simulation of contact force and speed relationship

```
v=linspace(0,70);

Fmax=0.00228*v.^2+60;

F=70;

plot(v,Fmax,'Red',v,F,'blue','linewidth',1.5),grid on

xlabel('speed in km/h')

ylabel('Contact Force in N')
```